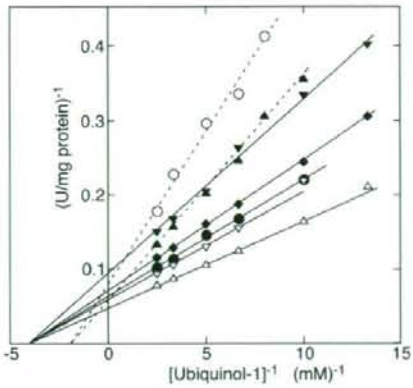

Fig. 4. Effects of antibiotics LL-Z1272 on kinetic parameters for Q_1H_2 oxidation by trypanosome AOX. Kinetic analysis was carried out in the absence of inhibitors (△) and the presence of 200 nM LL-Z1272β (▼), 20 nM LL-Z1272γ (●), 50 nM LL-Z1272δ (▲), 1 μM LL-Z1272ε (○) and 50 nM LL-Z1272ζ (▽), and 5 nM AF (◆). For clarity we showed data for one concentration of each inhibitor. The apparent K_m and V_{max} values determined for the control were 232 μM and 19.8 U/mg protein, respectively. The apparent K_i values for non-competitive inhibition by LL-Z1272β, γ, ζ, and AF were 142, 59, 203, and 2.65 nM. K_i and K_i' values for mixed-type inhibition by LL-Z1272δ and LL-Z1272ε were 0.032 and 25.5 μM and 0.483 and 9.61 μM, respectively.

and apparent K_m and V_{max} values were determined to be 232 μM and 20 U/mg protein (Fig. 4). The K_m value in 0.1% sucrose monolaurate was comparable to 350 μM for *T. b. brucei* AOX in 0.25% *n*-octyl-β-D-glucopyranoside *plus* 0.025% EDT-20 [34], but smaller than approximately 700 μM determined for *T. b. brucei* AOX in the absence of detergents [13,23]. Since the K_m value of *T. vivax* AOX for ubiquinol-2 was 116 μM (data not shown), the length of the isoprene unit may increase the binding affinity for ubiquinones [35]. The K_m of trypanosome AOX for ubiquinol-9 in *T. b. brucei* mitochondria would be comparable to the K_m value of cytochrome *bd* for ubiquinol-8 in *E. coli*.

Kinetic analysis of inhibition of *T. vivax* AOX by antibiotics LL-Z1272 revealed that LL-Z1272β (K_i=142 nM), γ (59 nM), and ζ (203 nM) act as (apparently) non-competitive inhibitors (Fig. 4), as reported for AF [13] and salicylhydroxamic acid (SHAM, K_i=25 μM) [34]. Since the amount of active AOX molecules in the *E. coli* membranes was difficult to estimate, we did not try kinetic analysis for tight-binding inhibitors [36]. In contrast, LL-Z1272δ and ε serve as mixed-type inhibitors with K_i and K_i' values of 0.032 and 25.5 μM and 0.483 and 9.61 μM, respectively.

4. Discussion

From the screening of natural antibiotics of the Kitasato Institute for Life Sciences Chemical Library, we identified prenylphenols LL-Z1272β, γ, δ, ε and ζ as a unique set of inhibitors, which can inhibit and discriminate bacterial and trypanosomal ubiquinol oxidases (Table 1). LL-Z1272β and ε (dechlorinated derivatives) inhibited cytochrome *bd*-type oxidase while LL-Z1272γ, δ, and ζ (chlorinated derivatives) were potent inhibitors of cytochrome *bo*-type oxidase and trypanosome AOX. Aurachin C is a potent inhibitor for both cytochrome *bo* and *bd* [20,27], while AF is more active against trypanosome AOX [13]. Since all three quinol oxidases are absent from mammalian mitochondria, prenylphenols could be used as lead compounds for development of novel chemotherapeutic agents [13,14,37]. However, except for the effect of LL-Z1272β on *Clostridium perfringens* (minimum inhibitory concentration of 25 μg/ml), antibiotics LL-Z1272 were ineffective against *S. aureus*, *Pseudomonas aeruginosa*, *Mycobacterium smegmatis*, and *Bacteroides fragilis*. Neither LL-Z1272γ nor LL-Z1272ε affected the aerobic growth of *E. coli* cells expressing cytochrome *bo* or *bd* as the sole terminal oxidase, likely due to the excretion by drug efflux pumps or due to the inefficient penetration through the lipopolysaccharide layer of the outer membrane.

Kinetic analysis of the inhibition of quinol oxidases by prenylphenols yielded rather complicated inhibition mechanisms (Figs. 2–4). Structural similarities of prenylphenols to ubiquinones (Fig. 1) indicate that all these compounds would act as competitive inhibitors for the quinol oxidation site. However, in many cases we found non-competitive or mixed type inhibition. In the case of tight binding inhibitors [36], Michaelis–Menten plots resemble to those of non-competitive inhibition. Alternatively, orientation of the phenol ring of prenylphenol molecules within the binding pocket will determine interactions of prenyl tails and/or the cyclohexanone ring with the protein moiety. The latter interactions would affect the former interactions. In addition, modifications of the prenyl tail (*i.e.*, the presence of the cyclohexanone or franone ring) could alter interactions with lipid bilayers and detergent micelles, which would then affect the orientation of inhibitor molecules relative to the binding pocket in quinol oxidases. Inhibition mechanisms of natural antibiotics may be inherently associated with their structural complexity, as found for inhibitors for alternative NADH dehydrogenase NDH-II [38].

Currently approved drugs for the treatment of human sleeping sickness caused by *T. b. rhodesiense* and *T. b. gambiense* are suramine, pentamidine, melarsoprol, and eflornithine [37]. They are not available for oral administration and *T. brucei* strains resistant to one or more drugs are now emerging. Thus there is an urgent need for less-toxic and more convenient new drugs against African trypanosomiasis. In parallel studies, we recently found trypanocidal activity of LL-Z1272β [39]. LL-Z1272β and LL-Z1272δ have been shown to be less toxic to human cells [18,33] and we have demonstrated that the efficacy of AF in the treatment of trypanosome-infected mice [14]. In conclusion, antibiotics LL-Z1272 are useful as probes for understanding the quinol oxidation sites of respiratory quinol oxidases and such prenylphenols are promising leading compounds for the development of new chemotherapeutic agents for African trypanosomiasis.

Acknowledgements

We thank Dr. M. Yamamoto (aRigen Pharmaceuticals. Inc., Tokyo) for AF, Dr. S. Yoshida (Institute of Physical and Chemical Research, Saitama) for piericidin A, Dr. Rokuro Masuma (Kitasato Institute for Life Sciences) for measurements of antibacterial activities of antibiotics LL-Z1272, Dr. K. Matsushita (Yamaguchi University) for his advice on enzyme assay and Dr. R. B. Gennis (University of Illinois) for the plasmid pNG2 and the *E. coli* strain GO103. This study was supported by a Grant-in-Aid for Scientific Research (20570124 to TM), Scientific Research on Priority Areas (18073004 to KK) and Creative Scientific Research (18GS0314 to KK) from the Japanese Ministry of Education, Science, Culture, Sports, and Technology.

References

[1] T.J. Foster, The *Staphylococcus aureus* "superbug", J. Clin. Invest. 114 (2004) 1693–1696.
[2] J. Travis, Reviving the antibiotic miracle? Science 264 (1994) 360–362.
[3] S. Jünneman, Cytochrome *bd* terminal oxidase, Biochim. Biophys. Acta 1321 (1997) 107–127.
[4] T. Mogi, M. Tsubaki, H. Hori, H. Miyoshi, H. Nakamura, Y. Anraku, Two terminal quinol oxidase families in *Escherichia coli*: variations on molecular machinery for dioxygen reduction, J. Biochem. Mol. Biol. Biophys. 2 (1998) 79–110.
[5] L. Cunningham, M. Pitt, H.D. Williams, The *cioAB* genes from *Pseudomonas aeruginosa* code for a novel cyanide-insensitive terminal oxidase related to the cytochrome *bd* quinol oxidases, Mol. Microbiol. 24 (1997) 579–591.
[6] S.S. Way, S. Sallustio, R.S. Magliozzo, M.B. Goldberg, Impact of either elevated or decreased levels of cytochrome *bd* expression on *Shigella flexneri* virulence, J. Bacteriol. 181 (1999) 1229–1237.

[7] S. Endley, D. McMurray, T.A. Ficht, Interruption of the *cydB* locus in *Brucella abortus* attenuates intracellular survival and virulence in the mouse model of infection, J. Bacteriol. 183 (2001) 2454–2462.
[8] A.K. Turner, L.Z. Barber, P. Wigley, S. Muhammad, M.A. Jones, M.A. Lovell, S. Hulme, P.A. Barrow, Contribution of proton-translocating proteins to the virulence of *Salmonella enterica* serovars Typhimurium, Gallinarum, and Dublin in chickens and mice, Infect. Immun. 71 (2003) 3392–3401.
[9] L. Shi, C.D. Sohaskey, B.D. Kana, S. Dawes, R.J. North, V. Mizrahi, M.L. Gennaro, Changes in energy metabolism of *Mycobacterium tuberculosis* in mouse lung and under *in vitro* conditions affecting aerobic respiration, Proc. Natl. Acad. Sci. U. S. A. 102 (2005) 15629–15634.
[10] M. Chaudhuri, R.D. Ott, G.C. Hill, Trypanosome alternative oxidase: from molecule to function, Trends Parasitol. 22 (2006) 484–491.
[11] A.L. Moore, M.S. Albury, P.G. Crichton, C. Affourtit, Function of the alternative oxidase: is it still a scavenger? Trends Plant Sci. 7 (2002) 478–481.
[12] N. Sasaki, T. Okutomi, T. Hosokawa, Y. Nawata, K. Ando, Ascofuranone, a new antibiotic from *Ascochyta viciae*, Tetrahedron Lett. 13 (1972) 2541–2544.
[13] N. Minagawa, Y. Yabu, K. Kita, K. Nagai, N. Ohta, K. Meguro, S. Sakajo, A. Yoshimoto, An antibiotic, ascofuranone, specifically inhibits respiration and in vitro growth of long slender bloodstream forms of *Trypanosoma brucei brucei*, Mol, Biochem. Parasitol. 84 (1997) 271–280.
[14] Y. Yabu, A. Yoshida, T. Suzuki, C. Nihei, K. Kawai, N. Minagawa, T. Hosokawa, K. Nagai, K. Kita, N. Ohta, The efficacy of ascofuranone in a consecutive treatment on *Trypanosoma brucei brucei* in mice, Parasitol. Int. 52 (2003) 155–164.
[15] H. Ui, A. Ishiyama, H. Sekiguchi, M. Namatame, A. Nishihara, A. Takahashi, K. Shiomi, K. Otoguro, S. Ō mura, Selective and potent *in vitro* antimalarial activities found in four microbial metabolites, J. Antibiot. 60 (2007) 220–222.
[16] S. Takamatsu, M.-C. Rho, R. Masuma, M. Hayashi, K. Komiyama, H. Tanaka, S. Omura, A novel testosterone 5a-reductase inhibitor, 8'9'-dehydroascochlorin produced by *Verticillium* sp. FO-2787, Chem. Pharm. Bull. 42 (1994) 953–956.
[17] G.A. Ellestad, R.H. Evans Jr., M.P. Kunstmann, Terpenoid metabolites from an unidentified *Fusarium* species, Tetrahedron 25 (1969) 1323–1334.
[18] S. Hayakawa, H. Minato, K. Katagiri, The ilicicolins, antibiotics from *Cylindrocladium ilicicola*, J. Antibiot. 24 (1971) 653–654.
[19] H. Minato, T. Katayama, S. Hayakawa, K. Katagiri, Identification of ilicicolins with ascochlorin and LL-Z1272, J. Antibiot. 25 (1972) 315–316.
[20] H. Miyoshi, K. Takegami, K. Sakamoto, T. Mogi, H. Iwamura, Characterization of the ubiquinol oxidation sites in cytochromes *bo* and *bd* from *Escherichia coli* using aurachin C analogues, J. Biochem. 125 (1999) 138–142.
[21] T. Mogi, S. Endo, S. Akimoto, M. Morimoto-Tadokoro, H. Miyoshi, Glutamates 99 and 107 in transmembrane helix III of subunit I of cytochrome *bd* are critical for binding of the heme b_{595}-*d* binuclear center and enzyme activity, Biochemistry 45 (2006) 15785–15792.
[22] M. Tsubaki, T. Mogi, Y. Anraku, H. Hori, Structure of heme–copper binuclear center of the cytochrome *bo* complex of *Escherichia coli*: EPR and Fourier-transform infrared spectroscopic studies, Biochemistry 32 (1993) 6065–6072.
[23] T. Suzuki, C. Nihei, Y. Yabu, T. Hashimoto, M. Suzuki, A. Yoshida, K. Nagai, T. Hosokawa, N. Minagawa, S. Suzuki, K. Kita, N. Ohta, Molecular cloning andcharacterization of *Trypanosoma vivax* alternative oxidase (AOX) gene, a target of the trypanocide ascofuranone, Parasitol. Int. 53 (2004) 235–245.
[24] T. Mogi, H. Ui, K. Shiomi, S. Ōmura, K. Kita, Gramicidin S identified as a potent inhibitor for cytochrome *bd*-type quinol oxidase, FEBS Lett. 582 (2008) 2299–2302.
[25] S. Jünemann, J.M. Wrigglesworth, Antimycin inhibition of the cytochrome *bd* complex from *Azotobacter vinelandii* indicates the presence of a branched electron transfer pathway for the oxidation of ubiquinol, FEBS Lett. 345 (1994) 198–202.
[26] K. Kita, K. Konishi, Y. Anraku, Terminal oxidases of *Escherichia coli* aerobic respiratory chain. II. Purification and properties of cytochrome b_{558}-*d* complex from cells grown with limited oxygen and evidence of branched electron-carrying systems, J. Biol. Chem. 259 (1984) 3375–3381.
[27] B. Meunier, S.A. Madgwick, E. Reil, W. Ottemeier, P.R. Rich, New inhibitors of the quinol oxidation sites of bacterial cytochromes *bo* and *bd*, Biochemistry 34 (1995) 1076–1083.
[28] Y. Matsumoto, E. Muneyuki, D. Fujita, K. Sakamoto, H. Miyoshi, M. Yoshida, T. Mogi, Kinetic mechanism of quinol oxidation by cytochrome *bd* studied with ubiquinone-2 analogs, J. Biochem. 139 (2006) 779–788.
[29] K. Kita, K. Konishi, Y. Anraku, Terminal oxidases of *Escherichia coli* aerobic respiratory chain. I. Purification and properties of cytochrome b_{562}-*o* complex from cells in the early exponential phase of aerobic growth, J. Biol. Chem. 259 (1984) 3368–3374.
[30] K. Matsushita, L. Patel, H.R. Kaback, Cytochrome *o* oxidase from *Escherichia coli*. Characterization of the enzyme and mechanism of electrochemical proton gradient generation, Biochemistry 23 (1984) 4703–4714.
[31] M. Sato-Watanabe, T. Mogi, H. Miyoshi, H. Iwamura, K. Matsushita, O. Adachi, Y. Anraku, Structure–function studies on the ubiquinol oxidation site of the cytochrome *bo* complex from *Escherichia coli* using *p*-benzoquinones and substituted phenols, J. Biol. Chem. 269 (1994) 28899–28907.
[32] T. Mogi, T. Hirano, H. Nakamura, Y. Anraku, Y. Orii, Cu_B promotes both binding and reduction of dioxygen at the heme–copper binuclear center in the *Escherichia coli bo*-type ubiquinol oxidase, FEBS Lett. 370 (1995) 259–263.
[33] M. Gutiérrez, C. Theoduloz, J. Rodríguez, M. Lolas, G. Schmeda-Hirschmann, Bioactive metabolites from the fungus *Nectria galligena*, the main apple canker agent in Chile, J. Agric. Food Chem. 53 (2005) 7701–7708.
[34] R. Ott, K. Chibale, S. Anderson, A. Chipeleme, M. Chaudhuri, A. Guerrah, N. Colowick, G.C. Hill, Novel inhibitors of the trypanosome alternative oxidase inhibit *Trypanosoma brucei brucei* growth and respiration, Acta Trop. 100 (2006) 172–184.
[35] K. Sakamoto, H. Miyoshi, M. Ohshima, K. Kuwabara, K. Kano, T. Akagi, T. Mogi, H. Iwamura, Role of isoprenyl tail of ubiquinone in reaction with respiratory enzymes: studies with bovine heart mitochondrial complex I and *Escherichia coli bo*-type ubiquinol oxidase, Biochemistry 37 (1998) 15106–15113.
[36] P.R. Rich, S.A. Madgwick, D.A. Moss, The interactions of duroquinol, DBMIB and NQNO with the chloroplast cytochrome *bf* complex, Biochim. Biophys. Acta 1058 (1991) 312–328.
[37] A.H. Fairlamb, Chemotherapy of human African trypanosomiasis: current and future prospect, Trends Parasitol. 19 (2003) 488–494.
[38] T. Mogi, K. Matsushita, H. Miyoshi, H. Ui, K. Shiomi, S. Ōmura, K. Kita, Identification of new inhibitors for alternative NADH dehydrogenase (NDH-II). FEMS Microbiol. Lett. (in press).
[39] K. Otoguro, A. Ishiyama, M. Namatame, A. Nishihara, T. Furusawa, R. Masuma, K. Shiomi, Y. Takahashi, H. Yamada, S. Omura, Selective and potent *in vitro* antitrypanosomal activities of ten microbial metabolites, J. Antibiot. 61 (2008) 372–378.

Glossary

AOX: alternatice quinol oxidase
HQNO: 2-heptyl-4-hydroxyquinoline *N*-oxide
IC_{50}: IC_{50}, the 50% inhibitory concentration
Q_1H_2: a reduced form of Q_1, ubiquinol-1

J. Biochem. 2009;145(2)229–237
doi:10.1093/jb/mvn161

Mitochondrial Dehydrogenases in the Aerobic Respiratory Chain of the Rodent Malaria Parasite *Plasmodium yoelii yoelii*

Kenji Kawahara[1], Tatsushi Mogi[1,*], Takeshi Q Tanaka[1], Masayuki Hata[1], Hideto Miyoshi[2] and Kiyoshi Kita[1,†]

[1]Department of Biomedical Chemistry, Graduate School of Medicine, the University of Tokyo, Hongo, Bunkyo-ku, Tokyo 113-0033; and [2]Division of Applied Life Sciences, Graduate School of Agriculture, Kyoto University, Sakyo-ku, Kyoto 606-8502, Japan

Received October 7, 2008; accepted November 19, 2008; published online December 6, 2008

In the intraerythrocytic stages of malaria parasites, mitochondria lack obvious cristae and are assumed to derive energy through glycolysis. For understanding of parasite energy metabolism in mammalian hosts, we isolated rodent malaria mitochondria from *Plasmodium yoelii yoelii* grown in mice. As potential targets for antiplasmodial agents, we characterized two respiratory dehydrogenases, succinate:ubiquinone reductase (complex II) and alternative NADH dehydrogenase (NDH-II), which is absent in mammalian mitochondria. We found that *P. y. yoelii* complex II was a four-subunit enzyme and that kinetic properties were similar to those of mammalian enzymes, indicating that the *Plasmodium* complex II is favourable in catalysing the forward reaction of tricarboxylic acid cycle. Notably, *Plasmodium* complex II showed IC_{50} value for atpenin A5 three-order of magnitudes higher than those of mammalian enzymes. Divergence of protist membrane anchor subunits from eukaryotic orthologs likely affects the inhibitor resistance. Kinetic properties and sensitivity to 2-heptyl-4-hydroxyquinoline-*N*-oxide and aurachin C of NADH: ubiquinone reductase activity of *Plasmodium* NDH-II were similar to those of plant and fungus enzymes but it can oxidize NADPH and deamino-NADH. Our findings are consistent with the notion that rodent malaria mitochondria are fully capable of oxidative phosphorylation and that these mitochondrial enzymes are potential targets for new antiplasmodials.

Key words: complex II, inhibitor, mitochondria, NDH-II, rodent malaria.

Abbreviations: AC, aurachin C; DCIP, 2,4-dichlorophenolindophenol; DHO, dihydroorotate; DHOD, DHO dehydrogenase; HQNO, 2-heptyl-4-hydroxyquinoline-*N*-oxide; hrCNE, high-resolution clear-native electrophoresis; IC_{50}, the 50% inhibitory concentration; NBT, nitro blue tetrazolium chloride; NDE, NDH-II bound to the outer surface of the mitochondrial inner membrane; NDI, NDH-II bound to the matrix side of the mitochondrial inner membrane; NQR, NADH:quinone reductase; Q_n, ubiquinone-n; SDH, succinate dehydrogenase; SQR, succinate:quinone reductase; TCA, tricarboxylic acid.

INTRODUCTION

Malaria remains one of the main global health problems, causing more than 1 million deaths per year, with about 90% of deaths and 60% of cases occurring in Africa, south of the Sahara (*1*). Mortality associated with malaria is mainly caused by the erythrocytic stage cells of human malaria *Plasmodium falciparum*. The emerging resistance against established drugs in *Plasmodium* populations (*2*) emphasizes the urgent need for the development of new antiplasmodial drugs.

Energy metabolism of *Plasmodium* is quite different from that of mammalian hosts. Intraerythrocytic stages of parasites have been considered for a long time to rely on incomplete oxidation of glucose with secretion of end products such as lactate and pyruvate (*3*) and to possess mitochondria that lack oxidative phosphorylation and a functional tricarboxylic acid (TCA) cycle (*4*, *5*). *Plasmodium* spp. lacks genes coded for the proton-translocating NADH dehydrogenase (NDH-I, complex I) present in mammalian mitochondria (*6*, *7*) and uses a rotenone-insensitive single-subunit NADH dehydrogenase (NDH-II) (*8*), which is assumed not to oxidize deamino-NADH (*9*). Succinate:ubiquinone oxidoreductase (complex II, succinate dehydrogenase (SDH)) is a membrane-bound TCA cycle enzyme and consists of four subunits: a flavoprotein subunit (Fp, SDH1) and an iron–sulphur subunit (Ip, SDH2) form a soluble heterodimer, which binds to a membrane anchor *b*-type cytochrome [CybL (SDH3)/CybS (SDH4) heterodimer]. The *Plasmodium SDH1* and *SDH2* genes have been cloned by homology probing (*10*) while SDH3 and SDH4 appear highly divergent from orthologs and are still not annotated in the current database (*6*, *7*). Membrane bound subuniuts *a* and *b* of ATP synthase also remain unidentified (*6*, *7*), and thus complete mitochondrial ATP synthase was assumed to be absent in *Plasmodium* spp. (*4*, *5*, *11–13*). Recently, Painter *et al.* (*13*) claimed that

*To whom correspondence addressed. Tel: +81-3-5841-3526, Fax: +81-3-5841-3444, E-mail: tmogi@m.u-tokyo.ac.jp
†Correspondence may also be addressed. Tel: +81-3-5841-3526, Fax: +81-3-5841-3444, E-mail: kitak@m.u-tokyo.ac.jp

the mitochondrial respiratory chain is required only for the regeneration of an oxidized form of ubiquinone, which serves as the electron acceptor for type 2 dihydroorotate dehydrogenase (DHOD), an essential enzyme for pyrimidine biosynthesis. It is widely accepted that the majority of the parasite's ATP demand is met through glycolysis (*11*).

On the contrary, atovaquone, an inhibitor for ubiquinol:cytochrome *c* reductase (complex III) (*14*), showed the antiplasmodial activity for *P. falciparum* with the 50% inhibitory concentration (IC_{50}) of 1 nM (*15*) and collapsed the mitochondrial membrane potential in *P. yoelii yoelii* (*16*). Uyemura *et al.* (*8*, *17*) demonstrated oxidative phosphorylation and succinate respiration in trophozoites of rodent malaria parasites. These observations suggest that *Plasmodium* mitochondria possess all subunits for canonical complex II and ATP synthase and are fully capable of oxidative phosphorylation.

It was shown recently that metabolism in *P. falciparum* parasites grown in human patients is affected by varied oxygen and substrate levels and by host-parasite interactions (*18*). The authors found the induction of gene sets associated with oxidative phosphorylation including respiratory enzymes. For understanding energy metabolism in malaria parasites, the isolation of active mitochondria from parasites, which have been adapted to host environments, is essential. In this study, *P. y. yoelii* mitochondria were isolated from parasites grown in mouse erythrocytes and enzymatic properties of complex II and NDH-II were characterized. Two-dimensional PAGE analysis supports the presence of membrane anchors in *Plasmodium* complex II. These findings indicate that *Plasmodium* mitochondria are fully capable of succinate-dependent oxidative phosphorylation as suggested by previous observations (*8*, *17*). Because the difference in the inhibitor sensitivity of complex II between *Plsamodium* and mammalian enzymes and the absence of NDH-II in mammalian mitochondria, these two enzymes are promising targets for new antimaralials.

MATERIALS AND METHODS

Parasite Culture—Animal care and experimental procedures were performed according to the Guidelines for Animal Experimentation, the University of Tokyo. *P. y. yoelii* strain 17XL was a kind gift of H. Otsuki (Ehime University). This strain can rapidly propagate without cerebral malaria and does not infect reticulocytes. About 3.0×10^7 parasites were injected intraperitoneally to 8-week-old female BALB/c mice, and the developmental stage and parasitemia were monitored by examination of Giemsa-stained thin blood smears. About 7.5 ml of the blood was collected from 10 mice by cardiac puncture 130–140 h after infection. To remove leukocytes and platelets, the blood was mixed with 0.5 ml of heparine and passed over a powdered cellulose column (CF11; Whatman, Clifton; 0.5 ml/ml blood), which has been equilibrated with 20 ml of PBS (*19*). Erythrocytes were eluted with 30 ml of PBS and collected by centrifugation at 4°C at $800 \times g$ for 5 min. In control experiments with uninfected mice, microscopic observations and examination of complex II and dihydroorotate dehydrogenase (DHOD) activities excluded the possible contamination of mouse leukocytes in the eluate. Erythrocytes were washed three times with RPMI-1640 medium (Gibco) and then transferred to RPMI-1640 medium supplemented with 10% AlbuMax I (Gibco) at the hematoclit of 3%. Then erythrocytes were incubated at 37°C for 2 h under conditions of 90% N_2, 5% O_2 and 5% CO_2, and trophozoite-rich parasites were recovered by centrifugation as above.

Preparation of Mitochondria—To isolate parasites, infected erythrocytes were lysed for 10 min on ice with 0.1% (w/v) saponin and the lysate was centrifuged at 4°C at $2,380 \times g$ for 10 min to remove erythrocyte membranes. Parasites were washed twice with PBS by centrifugation at 4°C at $5,800 \times g$ for 10 min and resuspended with 10–20 ml of buffer A [225 mM mannitol, 75 mM sucrose, 5 mM $MgCl_2$, 5 mM KH_2PO_4, 5 mM HEPES, 1 mM EGTA (pH 7.4)], supplemented with 0.1% (w/v) fatty acid-free bovine serum albumin (PAA Cell Culture Co.), 1 mM phenylmethanesufonyl fluoride (Sigma) and 1 × Protease Inhibitor Cocktail for general use (Sigma). Parasites were disrupted by N_2 cavitation at 1,200 psi for 20 min with 4639 Cell Disruption Bomb (Parr, USA) (*20*). Lysate was centrifuge at 4°C at $700 \times g$ for 8 min, and the resultant precipitate containing unbroken parasites was resuspended with 10 ml of buffer A and disrupted as above. This procedure was repeated twice to improve the parasite yield. Crude mitochondria were recovered from the supernatant by centrifugation at 4°C at $10,000 \times g$ for 8 min and suspended in buffer A at ~5 mg protein/ml. Rat liver mitochondria were prepared as described by Johnson and Lardy (*21*).

Enzyme Assay—Enzyme assay was performed at 25°C with V-660 double monochromatic spectrophotometer (JASCO, Tokyo, Japan; <0.00005 Abs noise) or UV-3000 double wavelength spectrophotometer (Shimadzu Corp., Kyoto, Japan), and reactions were started by addition of substrates (electron donors). Succinate:quinone reductase (SQR) activity was determined as quinone-mediated succinate:2,4-dichlorophenolindophenol (DCIP) reductase in 50 mM potassium phosphate (pH 8.0) containing 10 mM potassium succinate, 100 μM ubiquinone-2 (Q_2) and 45 μM DCIP ($\varepsilon_{600} = 21\ mM^{-1}\ cm^{-1}$) in the presence of 2 mM KCN. NADH:ubiquinone reductase (NQR) activity was measured in 50 mM potassium phosphate (pH 8.0) containing 200 μM NADH ($\varepsilon_{340} = 6.22\ mM^{-1}\ cm^{-1}$) and 100 μM ubiquinone-1 (Q_1) in the presence of 10 μM atovaquone and 2 mM KCN (*15*). DHOD activity was measured as DHO:DCIP reductase in 30 mM Tris–HCl (pH 8.0) containing 500 μM DHO, 100 μM Q_2 and 45 μM DCIP in the presence of 2 mM KCN (*20*). DHO:cytochrome *c* reductase activity was determined with 20 μM horse cytochrome *c* ($\varepsilon_{550} = 19\ mM^{-1}\ cm^{-1}$) in place of 45 μM DCIP (*20*). For inhibition studies, the reaction mixture was preincubated for 5 min in the presence of 0.1% (w/v) sucrose monolaurate (Mitsubishi-Kagaku Foods Co., Tokyo, Japan) to disperse hydrophobic substrates and inhibitors. Kinetic analysis and the estimation of the 50% inhibitory concentration (IC_{50}) were performed as described previously (*22*).

Clear-Native Electrophoresis and Activity Staining—Mitochondria were precipitated at 4°C at 20,400 × *g* for 5 min and resuspended at 6 mg protein/ml in 10 mM Tris–HCl (pH 7.4) containing 1% sucrose monolaurate, 1 mM sodium malonate and Protease Inhibitor Cocktail by brief sonication. After 20 min incubation at 4°C with rotating, the mixture was centrifuged at 4°C at 107,000 × *g* for 30 min and supernatant was concentrated at 4°C at 4,000 × *g* with Nanosep ultrafiltration devices (MWCO 100,000, Pall Life Science). Solubilized mitochondrial proteins were subjected to high resolution clear-native electrophoresis (hrCNE) (*23*) with 3–12% Novex gels (Invitrogen) using 0.02% dodecylmaltoside and 0.05% sodium deoxycholate for the cathode buffer additives. Gels were incubated at 25°C for 10 min in 30 mM Tris–HCl (pH 7.4) containing 20 mM potassium succinate and 0.5 mM nitro blue tetrazolium chloride (NBT), and then complex II band was visualized by 1 h incubation in dark in the presence of 0.2 mg/ml phenazine methosulphate. Protein bands were stained with GelCode (Pierce).

Analysis of Membrane Anchor Subunits of Complex II—Complex II bands identified as succinate:NBT reductase in hrCNE were cut out from gels and equilibrated with an equal amount of 2× SDS–PAGE sample buffer. Gel pieces were applied to 10–20% Supersep gels (Wako Pure Chemicals, Tokyo, Japan) and SDS–PAGE analysis was carried out. Protein bands were visualized by silver staining.

Miscellaneous—Protein contents of mitochondria and solubilized membrane proteins were determined with BIO-RAD and BCA protein assay reagent (Pierce), respectively, using bovine serum albumin as standard. Western blot analysis was carried out using anti-*P. falcifaum* (Pf) Fp and anti-PfIp rabbit antiserum and cross-reacted bands were visualized by alkaline phosphatase-conjugated anti-rabbit IgG (Bio-Rad) (*24*).

RESULTS

Preparation of Plasmodium Mitochondria—After infection of mice with rodent malaria parasites, we monitored amounts of erythrocytes and parasitemia and found that the number of parasites decreased sharply 140 h after infection as the number of the erythrocyte decreased. Thus, we collected the infected blood 130 to 140 h after infection. Leukocyte-free washed erythrocytes were incubated at 37°C for 2 h in RPMI-1640 medium supplemented with 10% AlbuMax I to adjust the developmental stage to trophozoites (trophozoite : ring : schizont = 7 : 2 : 1). Then the parasites were released from infected erythrocytes with 0.1% saponin and disrupted by the N_2 cavitation method (*20*).

Yield of Plasmodium Mitochondria—SQR activity and DHOD activity of *P. y. yoelii* mitochondria were 5- and 3-fold, respectively, higher than those of the axenic cultured *P. falciparum* (*20*). Furthermore, yields of mitochondrial proteins (5.5 ± 1.3 mg protein) and total activities of complex II (56 ± 14 mU) and DHOD (132 ± 18 mU) after preparation from ten infected mice were much greater than those of *P. falciparum* mitochondria [1 mg protein, 2 mU (*25*), and 7 mU (*20*), respectively, from the 360-ml *in vitro* culture]. Thus, in terms of the yield and specific activity, *P. y. yoelii* mitochondria are suitable for biochemical studies on mitochondrial enzymes of malaria parasites.

Table 1. **Enzymatic properties of *P. y. yoelii* mitochondria.**

Enzyme	Specific activity (mU/mg protein)	
	P. y. yoelii[a]	Rat liver
Succinate:DCIP reductase (complex II)	2.66 ± 0.02	188
NADH:Q_1 reductase[b]	42.2 ± 0.3	152
NADH:Cyt *c* reductase[c]	18.6 ± 1.6	ND[d]
DHO:DCIP reductase (DHOD)	10.5 ± 1.3	2.6
Q_1H_2 oxidase (complex III + complex IV)	19.4 ± 0.2	166

[a]Values were mean ± SD. Freshly prepared *P. y. yoelii* mitochondria showed SQR, NQR and DHOD activities of 10.2 ± 0.1, 63.2 ± 10.1 and 24.1 ± 3.9 mU/mg protein (n = 6), respectively. Enzyme activities were reduced to about one half after freeze-thaw of mitochondria preparations, which have been stored at −80°C. [b]NDH-II of *P. y. yoelii* or NDH-I of rat liver mitochondria were analysed. [c](NDH-II of *P. y. yoelii* or NDH-I of rat liver mitochondria) + complex III were analysed. [d]ND, not determined.

Comparison of Mitochondrial Enzymes from P. y. yoelii and Rat Liver—When comparing with rat liver mitochondria, SQR (complex II), NQR (NDH-II) and Q_1H_2 oxidase (complex III *plus* complex IV) activity of *P. y. yoelii* mitochondria were 1.4%, 28% and 12%, respectively, of rat liver mitochondria whereas DHOD activity was 4-fold higher than that of rat liver mitochondria (Table 1). Rotenone [IC_{50} = 13 nM for bovine complex I (*26*)] inhibited rat liver mitochondria complex I 95–97% at 1 μM while the inhibition of the *P. y. yoelli* NQR activity by 10 μM rotenone was only 20%. Since NQR activity of *P. y. yoelii* mitochondria followed a simple Michaelis–Menten kinetics (see below), we concluded that the enzyme activities are not due to contaminated mouse mitochondria derived from leukocytes or platelets.

Enzymatic Properties of Plasmodium Complex II—SQR activity of *P. y. yoelii* mitochondria displayed Michaelis–Menten kinetics (Fig. 1). Apparent K_m values for succinate and Q_2 were estimated to be 49 and 0.17 μM, respectively, which are close to 20 and 0.5 μM, respectively, of bovine complex II (*27*). Apparent K_m value for Q_1 was found to be 1.6 μM. Differences in K_m value (9-fold) and V_{max}/K_m ratio (19-fold) between Q_1 and Q_2 indicate that the 6-polyprenyl tail of the ubiquinone ring contributes to the binding affinity and that Q_2 is better substrate than Q_1.

Then effects of the quinone-binding site inhibitors on the SQR activity were examined. Atpenin A5 and carboxin are known inhibitors for bovine complex II with IC_{50} values of 4 nM and 1 μM, respectively (*28*) and plumbagin (5-hydroxy-2-methyl-1,4-naphthoquinone) has been reported to inhibit *P. falciparum* complex II (IC_{50} = 5 μM) and the growth (IC_{50} = 0.27 μM) (*29*). At 100 μM Q_2, we found that IC_{50} values for atpenin A5 and carboxin were 4.6 and 3.6 μM, respectively, in *P. y. yoelii* mitochondria and 7.1 nM and 3.8 μM, respectively, in rat liver mitochondria (Fig. 2). The inhibition by plumbagin was only 50% even at 100 μM.

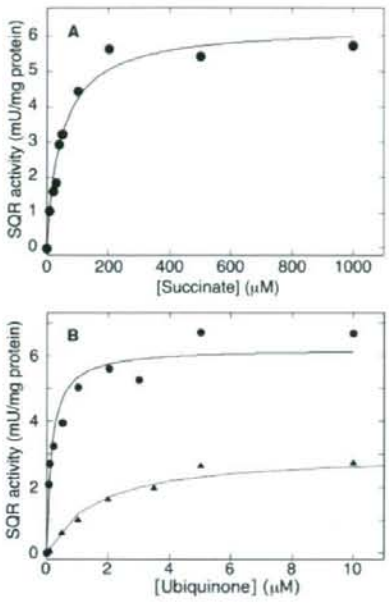

Fig. 1. **Kinetic analysis of SQR activity of *P. y. yoelii* mitochondria.** (A) As a function of the succinate concentration, SQR activity was examined at 6 μg mitochondrial protein/ml in the presence of 0.1 mM Q_2. Data points were averages from three independent preparations (6.19 ± 0.93 mU/mg protein with 1 mM succinate and 0.1 mM Q_2). Data were fitted to Michaelis–Menten kinetics with apparent K_m and V_{max} values of 49.3 ± 7.0 μM and 6.26 ± 0.27 mU/mg protein, respectively. (B) As a function of the Q_1 (circles) or Q_2 (triangles) concentration, SQR activity was examined in the presence of 10 mM succinate. Data points were averages from two independent preparations (6.25 ± 0.87 mU/mg protein with 1 mM succinate and 0.1 mM Q_2). Data were fitted to Michaelis–Menten kinetics with apparent K_m and V_{max} values of 1.61 ± 0.20 μM and 3.03 ± 0.12 mU/mg protein, respectively, for Q_1 and 0.17 ± 0.04 μM and 6.20 ± 0.30 mU/mg protein, respectively, for Q_2.

Membrane Anchor Subunits of Plasmodium Complex II—For reduction of ubiquinone, *Plasmodium* complex II should have a quinone-binding pocket provided by Ip and the CybL/CybS heterodimer (*30–32*). For the examination of subunit structure of *Plasmodium* complex II, we first determined the molecular weight of *P. y. yoelii* complex II by hrCNE, followed by in-gel activity staining as phenazine methosulphate-mediated succinate : NBT reductase. An apparent molecular weight of *P. y. yoelii* complex II was estimated to be 135 kDa (Fig. 3, lane 2), which is comparable to 130 kDa of bovine and yeast complex II (*33*). Western blot analysis identified Fp and Ip as the 70- and 35-kDa proteins, respectively (Fig. 3, lanes 3 and 4), indicating that a sum of molecular weights of membrane anchor subunits is about 30 kDa. Subsequently, the 135-kDa bands in hrCNE were excised from gels and subjected to SDS–PAGE analysis. Due to an extremely low activity of *Plasmodium* complex II (~1% of mammalian mitochondria) and the diffusion of a reduced product of NBT, it was difficult to cut out the complex II band but we were able to identify 70, 35, 16 and 14 kDa bands as putative subunits of the 135-kDa complex (Fig. 3, lane 5).

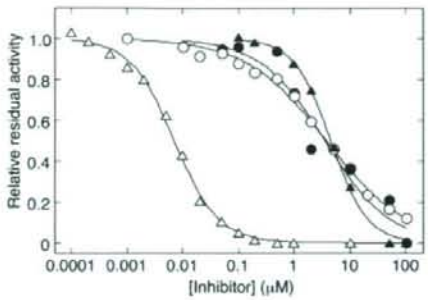

Fig. 2. **Inhibition of SQR activity of *P. y. yoelii* mitochondria by atpenin A5 and carboxin.** SQR activity of *P. y. yoelii* (closed symbols) and rat liver (open symbols) mitochondria was determined with 10 mM potassium succinate and 0.1 mM Q_2 in the presence of atpenin A5 (triangles), and carboxin (circles). Data points were average values from two independent preparations. IC_{50} values were determined to be 4.6 ± 0.2 μM for atpenin A5 and 3.6 ± 1.0 μM for carboxin in *P. y. yoelii* mitochondria and 7.1 ± 0.3 nM for atpenin A5 and 3.8 ± 0.1 μM for carboxin in rat liver mitochondria. Control activitiy of *P. y. yoelii* mitochondria was 2.68 ± 0.03 mU/mg protein.

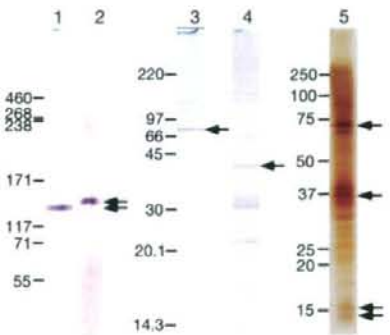

Fig. 3. **Electrophoresis analysis of complex II in *P. y. yoelii* mitochondria.** Solubilized mitochondrial proteins were subjected to hrCNE, and complex II of bovine (lane 1, 2.4 μg protein) and *P. y. yoelii* (lane 2, ~0.4 mg protein) mitochondria were visualized by SDH activity staining. Arrows indicate complex II bands. For Western blot analysis, 10 μg of mitochondrial proteins were subjected to 15% SDS–PAGE and Fp (lane 3) and Ip (lane 4), indicated by arrows, were identified by anti-PfFp and anti-PfIp rabbit antisera, respectively. For identification of *P. y. yoelii* complex II subunits, complex II bands in hrCNE were excised from gels and subjected to 10–20% SDS–PAGE, followed by silver staining (lane 5). Putative subunits of *P. y. yoelii* complex II are indicated by arrows. HiMark Prestained High Molecular Weight Protein Standard (Invitrogen), Rainbow Colored Protein Molecular Weight Marker (High molecular weight range) (Amersham Pharmacia Biotech), and Precision Plus Protein Standard (Bio-Rad) were used as molecular weight standards for lanes 1 and 2, lanes 3 and 4, and lane 5, respectively.

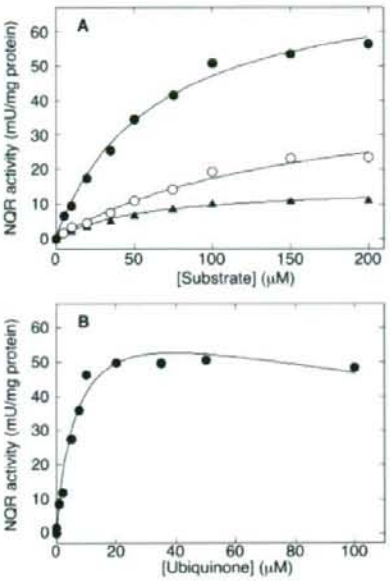

Fig. 4. **Kinetic analysis of NQR activity in *P. y. yoelii* mitochondria.** (A) As a function of the concentration of NADH (closed circle), NADPH (open circle) or deamino-NADH (closed triangle), NQR activity was examined at 6 μg protein/ml in the presence of 0.1 mM Q_1. Data points were averages from two independent preparations (44.9 ± 4.8 mU/mg protein with 0.2 mM NADH). Data were fitted to Michaelis–Menten kinetics with apparent K_m and V_{max} values of 63.2 ± 6.9 μM and 76.7 ± 3.4 mU/mg protein, respectively, for NADH, 157 ± 33 μM and 44.4 ± 5.4 mU/mg protein, respectively, for NADPH, 58.4 ± 5.7 μM and 15.1 ± 0.6 mU/mg protein, respectively, for deamino-NADH. (B) As a function of the concentration of Q_1, NQR activity was examined in the presence of 0.2 mM NADH. Data points were average values from two independent preparations [48.6 ± 7.9 mU/mg protein at 0.1 mM Q_1). Data were fitted to substrate inhibition kinetics with apparent K_m, V_{max} and K_{is} values of 7.2 ± 1.7 μM, 71.8 ± 7.6 mU/mg protein, and 218 ± 97 μM, respectively, using the equation $v = V_{max}$ $S/(K_m + S + S\ (1+S/K_{is}))$.

Enzymatic Properties of Plasmodium NDH-II—*Plasmodium* spp. lacks genes encoding complex I (*6*, *7*) and uses a single-subunit NADH dehydrogenase (NDH-II) (*8*, *15*). Upon permealization of mitochondria with 30 μg/ml alamethicin, which forms pores large enough to permit the rapid diffusion of NADH (*34*), NQR and SQR activities increased 32% and 27%, respectively, indicating that *Plasmodium* NDH-II is likely located at the matrix side of the inner membrane.

When reactions were started by addition of NADH, NQR activity showed a simple Michaelis–Menten kinetics with apparent K_m and V_{max} values of 63 μM for NADH and 77 mU/mg protein, respectively (Fig. 4A). K_m value for NADH was closer to 31 μM of *Saccharomyces cerevisiae* internal NDH-II (NDI1) (*35*) and 34 μM of *E. coli* NDH-II (*36*) than 15 μM of yeast *Yarrowia lipolytica* external NDH-II (NDE) (*37*). In contrast,

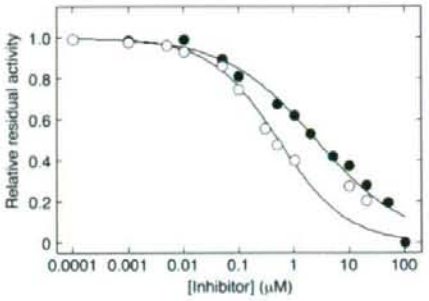

Fig. 5. **Inhibition of NQR activity of *P. y. yoelii* mitochondria by HQNO and Aurachin C1-10.** NQR activity of *P. y. yoelii* mitochondria was determined with 0.2 mM NADH and 0.1 mM Q_1 in the presence of HQNO (closed circle) or aurachin C1-10 (open circle). Data points were average values from two independent preparations. Control activity of *P. y. yoelii* mitochondria was 45.6 ± 1.3 mU/mg protein with 0.1 mM Q_1. IC_{50} values for HQNO and aurachin C1-10 were estimated to be 2.5 ± 0.4 and 0.47 ± 0.03 μM, respectively.

Q_1-started NQR activity showed substrate inhibition kinetics with K_m and K_{is} values of 7 and 218 μM, respectively, for Q_1 (Fig. 4B). Unlike *E. coli* NADH-II (*36*) and *Y. lipolytica* NDE (*37*), *P. y. yoelii* NDH-II can oxidize deamino-NADH (K_m = 58 μM, V_{max} = 15 U/mg protein) and NADPH (K_m = 157 μM, V_{max} = 44 mU/mg protein) (Fig. 5A). V_{max}/K_m ratios indicate that *Plasmodium* NDH-II is more specific to NADH compared to NAD(P)H dehydrogenases from red beet root mitochondria [NDI (*38*) and NDE (*39*)].

Since mammalian hosts lack NDH-II, this enzyme is a promising target for new antiplasmodial agents. However, inhibitors for NDH-II are rare and mostly unspecific (*34*). Fry *et al.* (*11*) examined effects of inhibitors on ATP level in erythrocytic *P. falciparum* and found that 2-heptyl-4-hydroxyquinoline *N*-oxide (HQNO) and 5-hydroxy-2-methyl-1,4-naphthoquinone (plumbagin) showed antimalarial activities with IC_{50} values of 4.0 and 3.5 μM, respectively. In yeast, quinolone analogues HQNO and aurachin C 0-11 were shown to inhibit NDI1 with the IC_{50} values of 8 and 0.2 μM, respectively (*40*). In this study, we examined effects of HQNO and aurachin C 1-10 (*41*) on NADH:Q_1 reductase activity and determined IC_{50} values to be 2.5 and 0.5 μM, respectively (Fig. 5). Our data indicate that the quinolone analogues are potent inhibitors for *Plasmodium* NDH-II. Trifluoroperazine, the uncompetitive inhibitor in terms of Q_2 for *Mycobacterium tuberculosis* NDH-II (IC_{50} = 12 μM) (*42*), reduced the NADH:Q_1 reductase activity to 26% of the control at 100 μM.

DISCUSSION

Properties of Plasmodium Complex II—Parasitic nematodes adapted to hypoxic host environments, have modified respiratory chain, where isoforms of complex II serve as fumarate reductase (*43*, *44*). Kinetic properties of *P. y. yoelii* complex II are similar to those of mammalian enzymes and thus suitable for catalysing the

Table 2. **Effects of quinone-binding site inhibitors on SQR activity of *P. y. yoelii* mitochondria.**

100 μM inhibitor	*P. y. yoelii* mitochondria	Rat liver mitochondria
Control	100%	100%
Atpenin A5	<0.4	<0.05
Carboxin	<0.4	<0.05
Flutoranil	58	22
TTFA	80	12
HQNO	54	94
Plumbagin	52	98
DNP-17	67	99

Control activities (mean ± SD) were 2.66 ± 0.02 (*P. y. yoelii*) and 180 ± 5 (rat liver) mU/mg protein.

forward reaction of TCA cycle (i.e. the oxidation of succinate). It should be noted that *Plasmodium* complex II was more resistant to known quinone-binding site inhibitors for mammalian complex II (Table 2), probably due to the divergence of membrane anchor subunits of *Plasmodium* complex II.

From the whole cell lysate of *P. falciparum*, Suraveratum *et al.* (*28*) purified complex II as the Fp/Ip heterodimer with an apparent molecular weight of 90 kDa and claimed that it has a much lower K_m value (3 μM) for succinate and plumbagin-sensitive SQR activity. However, the concentration (0.2%) of octyl glucoside used for the isolation of *P. falciparum* complex II was not enough for the solubilization of membrane proteins (i.e. critical micell concentration of octyl glucoside is 0.73%). Octyl glucoside likely dissociates the Fp/Ip dimer from the membrane anchor and the aerobic isolation of the Fp/Ip dimer would damage the iron–sulphur clusters in Ip. Thus, SQR activity of such preparations need to be carefully examined.

Plasmodium CybL and CybS are still not annotated in the current database (*6*, *7*), likely due to the divergence from ortholog sequences. However, 2D–PAGE analysis (Fig. 3), SQR activity (Fig. 1, refs. *20*, *25*) and the structure of quinone-binding site in complex II (*30–32*) support the presence of these membrane anchor subunits in *Plasmodium* spp. In membrane anchors of complex II, "$Rx_{16}Sx_2HR$" (helix I) and '$YHx_{10}D$' (helix II) motifs in CybL and '$LHx_{10}DY$' (helix II) motif in CybS are conserved for quinone/haem binding. And only such motifs are conserved in protist membrane anchors (*45*). One candidates for *P. y. yoelii* CybL (accession no. XP_731082, 10,086 Da) and one candidate for CybS (accession no. XP_726783, 10,379 Da) can be identified from 3,310 ORFs shared by *P. falciparum* and *P. y. yoelii* on the basis of the size (<200 amino acid residues), the presence of transmembrane segments (≤3), and the quinone/haem-binding motifs. PyCybL and PyCybS have two transmembrane regions and contain the quinone/haem-binding motifs, '$Rx_{14}Sx_2HY$' and '$YYx_{10}DY$' motifs and '$Yx_{10}G$' motif, respectively. In *S. cerevisiae* strain S288C (Baker's yeast), CybS (accession no. NP_010463) uses the $Yx_{10}DY$ motif, and the His-to-Tyr mutant of the CybL $YHx_{10}D$ motif retained a half of the enzyme activity and haem (*46*). Thus, in *Plasmodium* CybL and CybS, Tyr could also substitute the role of the conserved His residue in membrane anchor subunits. Although it has to be tested by protein chemically in future studies, our data support that the subunit structure of *Plasmodium* complex II is similar to that of mammalian complex II.

Properties of Plasmodium NDH-II—Previously, Krungkrai *et al.* (*47*) isolated mitochondrial complex I from *P. falciparum* and *P. berghei* as a 130-kDa complex containing 38- and 33-kDa subunits. They claimed that NADH:ubiquinone-8 reductase activity was sensitive to rotenone (IC_{50} = 12 μM) and plumbagin (IC_{50} = 6 μM). However, NDH-I is not encoded by the *Plasmodium* genomes (*6*, *7*) and concentrations of *n*-octyl glucoside used for the solubilization and purification were below its critical micelle concentration (CMC) where *n*-octyl glucoside cannot serve as a detergent. Alternative NADH dehydrogenase NDH-II is a rotenone-insensitive single-subunit enzyme (*15*, *34*) and the apparent molecular weights and subunit structure of *P. falciparum* (acc. no. XP_001352022 and MW 61,670) and *P. y. yoelii* (acc. no. XP_731423, MW 66,156) NDH-II are totally different from those reported by Krungkrai *et al.* (*47*). The IC_{50} value of mouse liver mitochondria for rotenone (8.4 μM; Table 3 in ref. 47) was three orders of magnitude higher than the IC_{50} reported for mammalian enzymes (*26*). Recently, Biagini *et al.* (*15*) used the whole cell lysate of *P. falciparum* and claimed that PfNDH-II was inhibited by diphenylene iodonium chloride (DPI, IC_{50} of 15–25 μM) and diphenyl iodonium chloride (IDP, IC_{50} = 66 μM). As pointed out by Vaidya *et al.* (*48*), the IC_{50} for the enzyme was 100- and 10-fold higher than those for the growth inhibition and other NADH oxidases in the lysate may contribute to the activity. Very recently, it was reported that purified recombinant PfNDH-II was not inhibited by known NDH-I inhibitors and flavoenzyme inhibitors (DPI and IDP) (Dong, C., Patel, V., Clardy, J., and Wirth, D., personal communication). Thus, previous studies on *Plasmodium* NDH-II need to be reexamined. Our data indicate that *Plasmodium* NDH-II is a member of internal NDH-II (Ndi), which reoxidizes NADH in the mitochondrial matrix. Recently, Saleh *et al.* (*49*) demonstrated the antiplasmodial activity (IC_{50} = 14 nM) of 1-hydroxy-2-dodecyl-4(1*H*)quinolone (HDQ), which has been identified as the potent inhibitor for *Y. lipolytica* NDE (IC_{50} = 0.2 μM) (*50*), demonstrating that *Plasmodium* NDH-II is a promising target for new drugs.

Oxidative Phosphorylation in Plasmodium Mitochondria—For a long time, it has been assumed that *Plasmodium* mitochondria cannot carry out oxidative phosphorylation (*4*, *5*) because of a lack of membrane anchor subunits of ATP synthase (*9*, *11*). Oxidative phosphorylation, succinate respiration (*8*, *17*), and effects of respiratory complex inhibitors on the generation of membrane potential (*16*) in rodent malaria mitochondria support the notion that *Plasmodium* mitochondria are fully capable of oxidative phosphorylation. Careful analysis of current genome databases (*6*, *7*) with partial subunits sequences of *Crithidia fasciculata* (*51*) and *Leishmania tarentolae* (*52*) could identify ten subunits of *P. falciparum* F_oF_1-ATP synthase, including membrane anchor subunits *a* (XP_001347344) and *b* (XP_001348969) (Mogi, T. and Kita, K., unpublished

results), which are found to be highly divergent from eukaryotic and bacterial counterparts. Thus, all canonical subunits of complex II and ATP synthase are present in *Plasmodium* spp., and malaria parasites can yield energy *via* oxidative phosphorylation. The *in vivo* expression profiles of parasites derived from infected patients showed the up-regulation of these enzymes under conditions similar to starvation in yeast (*18*).

CONCLUSION

We isolated active mitochondria from rodent malaria *P. y. yoelii* from infected mouse erythrocytes and characterized complex II and NDH-II. *Plasmodium* complex II is the four-subunit enzyme but its quinone-reduction site in the membrane anchor subunits seems structurally different from that of mammalian enzyme. *Plasmodium* NDH-II showed enzymatic properties similar to those of NDI and quinolones were found to be potent inhibitors. Alternative respiratory enzymes, which are absent in mammalian mitochondria, are as promising targets for new antibiotics (*53*, *54*). We hope that our findings will help understanding of energy metabolism in malaria parasites and the development of new antimalarial drugs.

FUNDING

This study was supported in part by a grant-in-aid for scientific research (20570124 to T.M.), scientific research on Priority Areas (18073004 to K.K.) and Creative Scientific Research (18GS0314 to K.K.) from the Japanese Ministry of Education, Science, Culture, Sports, and Technology. We thank Dr H. Ohtsuki (Ehime University) for *P. y. yoelii* strain 17XL, Dr. D. Wirth (Harvard School of Public Health) for the use of unpublished results prior to publication, and Ministry of Health, Labour and Welfare for financial supports.

CONFLICT OF INTEREST

None declared.

REFERENCES

1. World Health Organization (2007) Malaria Elimination. A field manual for low and moderate endemic countries. World Health Organization, Geneva, Switzerland
2. Hyde, J.E. (2005) Drug-resistant malaria. *Trends Parasitol.* **21**, 494–498
3. Sherman, I.W. (1998) Carbohydrate metabolism of asexual stages. in *Malaria, Parasite Biology, Pathogenesis and Protection* (Sherman, I.W., ed.), pp. 135–143, ASM Press, Washington, DC
4. Vaidya, A.B. (1998) Mitochondrial physiology as a target for atovaquone and other antimalarials. in *Malaria, Parasite Biology, Pathogenesis and Protection* (Sherman, I.W., ed.), pp. 355–368, ASM Press, Washington, DC
5. Van Dooren, G.G., Stimmler, L.M., and McFadden, G.I. (2006) Metabolic maps and functions of the *Plasmodium* mitochondrion. *FEMS Microbiol. Rev.* **30**, 596–630
6. Gardner, M.J., Hall, N., Fung, E., White, O., Berriman, M., Hyman, R.W., Carlton, J.M., Pain, A., Nelson, K.E., Bowman, S., Paulsen, I.T., James, K., Eisen, J.A., Rutherford, K., Salzberg, S.L., Craig, A., Kyes, S., Chan, M.S., Nene, V., Shallom, S.J., Suh, B., Peterson, J., Angiuoli, S., Pertea, M., Allen, J., Selengut, J., Haft, D., Mather, M.W., Vaidya, A.B., Martin, D.M., Fairlamb, A.H., Fraunholz, M.J., Roos, D.S., Ralph, S.A., McFadden, G.I., Cummings, L.M., Subramanian, G.M., Mungall, C., Venter, J.C., Carucci, D.J., Hoffman, S.L., Newbold, C., Davis, R.W., Fraser, C.M., and Barrell, B. (2002) Genome sequence of the human malaria parasite *Plasmodium falciparum*. *Nature* **419**, 498–511
7. Carlton, J.M., Angiuoli, S.V., Suh, B.B., Kooij, T.W., Pertea, M., Silva, J.C., Ermolaeva, M.D., Allen, J.E., Selengut, J.D., Koo, H.L., Peterson, J.D., Pop, M., Kosack, D.S., Shumway, M.F., Bidwell, S.L., Shallom, S.J., van Aken, S.E., Riedmuller, S.B., Feldblyum, T.V., Cho, J.K., Quackenbush, J., Sedegah, M., Shoaibi, A., Cummings, L.M., Florensk, L., Yatesk, J.R., Raine, J. D., Sinden, R.E., Harris, M.A., Cunningham, D.A., Preiser, P.R., Bergman, L.W., Vaidya, A.B., van Lin, L.H., Janse, C.J., Waters, A.P., Smith, H.O., White, O.R., Salzberg, S.L., Venter, J.C., Fraser, C.M., Hoffman, S.L., Gardner, M.J., and Carucci, D.J. (2002) Genome sequence and comparative analysis of the model rodent malaria parasite *Plasmodium yoelii yoelii*. *Nature* **419**, 512–519
8. Uyemura, S.A., Luo, S., Vieira, M., Moreno, S.N., and Docampo, R. (2004) Oxidative phosphorylation and rotenone-insensitive malate- and NADHquinone oxidoreductases in *Plasmodium yoelii yoelii* mitochondria *in situ*. *J. Biol. Chem.* **279**, 385–393
9. Matsushita, K., Ohnishi, T., and Kaback, H.R. (1987) NADH-ubiquinone oxidoreductases of the *Escherichia coli* aerobic respiratory chain. *Biochemistry* **26**, 7732–7737
10. Takeo, S., Kokaze, A., Ng, C.S., Mizuchi, D., Watanabe, J.I., Tanabe, K., Kojima, S., and Kita, K. (2000) Succinate dehydrogenase in *Plasmodium falciparum* mitochondria: molecular characterization of the *SDHA* and *SDHB* genes for the catalytic subunits, the flavoprotein (Fp) and iron–sulfur (Ip) subunits. *Mol. Biochem. Parasitol.* **107**, 191–205
11. Fry, M., Webb, E., and Pudney, M. (1990) Effect of mitochondrial inhibitors on adenosinetriphosphate levels in *Plasmodium falciparum*. *Comp. Biochem. Physiol. B* **96**, 775–782
12. Vaidya, A.B. and Mather, M.W.A. (2005) Post-genomic view of the mitochondrion in malaria parasites. *Curr. Top. Microbiol. Immunol.* **295**, 233–250
13. Painter, H.J., Morrisey, J.M., Mather, M.W., and Vaidya, A.B. (2007) Specific role of mitochondrial electron transport in blood-stage *Plasmodium falciparum*. *Nature* **446**, 88–91
14. Fry, M. and Pudney, M. (1992) Site of action of the antimalarial hydroxynaphthoquinone, 2-[trans-4-(4′-chlorophenyl)cyclohexyl]-3-hydroxy-1,4-naphthoquinone (566C80). *Biochem. Pharmacol.* **43**, 1545–1453
15. Biagini, G.A., Viriyavejakul, P., O'Neill, P.M., Bray, P.G., and Ward, S.A. (2006) Functional characterization and target validation of alternative Complex I of *Plasmodium falciparum* mitochondria. *Antimicrob. Agents Chemother.* **50**, 1841–1851
16. Srivastava, I.K., Rottenberg, H., and Vaidya, A.B. (1997) Atovaquone, a broad spectrum antiparasitic drug, collapses mitochondrial membrane potential in malarial parasite. *J. Biol. Chem.* **272**, 3961–3966
17. Uyemura, S.A., Luo, S., Moreno, S.N.J., and Docampo, R. (2000) Oxidative phosphorylation, Ca^{2+} transport, and fatty acid-induced uncoupling in malaria parasites mitochondria. *J. Biol. Chem.* **275**, 9709–9715
18. Daily, J.P., Scanfeld, D., Pochet, N., Roch, K.L., Plouffe, D., Kamel, M., Sarr, O., Mboup, S., Ndir, O., Wypij, D., Lavasseur, K., Thomas, E., Tamayo, P., Dong, C., Zhou, Y., Lander, E.S., Ndiaye, D., Wirth, D., Winzeler, E.A., Mesirov, J.P., and Regev, A. (2007)

Distinct physiological states of *Plasmodium falciparum* in malaria-infected patients. *Nature* **450**, 1091–1095
19. Homewood, C.A. and Neame, K.D. (1976) Comparison of methods used for removal of white cells from malaria-infected blood. *Ann. Trop. Med. Parasitol.* **70**, 249–251
20. Takashima, E., Takamiya, S., Takeo, S., Mi-ichi, F., Amino, H., and Kita, K. (2001) Isolation of mitochondria from *Plasmodium falciparum* showing dihydroorotate dependent respiration. *Parasitol. Int.* **50**, 273–278
21. Johnson, D. and Lardy, H. (1967) Isolation of liver or kidney mitochondria in *Methods Enzymol.* Vol. 10, (Estabrook, R.W. and Pullman, M.E., eds.), pp. 94–96, Academic Press, New York
22. Mogi, T., Ui, H., Shiomi, K., Ōmura, S., and Kita, K. (2008) Gramicidin S identified as a potent inhibitor for cytochrome *bd*-type quinol oxidase. *FEBS Lett.* **582**, 2299–2302
23. Wittig, I., Karas, M., and Schagger, H. (2007) High resolution clear native electrophoresis for in-gel functional assays and fluorescence studies of membrane protein complexes. *Mol. Cell Proteomics* **6**, 1215–1122
24. Kobayashi, T., Sato, S., Takamiya, S., Komaki-Yasuda, K., Yano, K., Hirata, A., Onitsuka, A., Hata, M., Mi-ichi, F., Tanaka, T., Hase, T., Miyajima, A., Kawazu, S., Watanabe, Y., and Kita, K. (2007) Mitochondria and apicoplast of *Plasmodium falciparum*: behaviour on subcellular fractionation and the implication. *Mitochondrion* **7**, 125–132
25. Mi-Ichi, F., Miyadera, H., Kobayashi, T., Takamiya, S., Waki, S., Iwata, S., Shibata, S., and Kita, K. (2005) Parasite mitochondria as a target of chemotherapy: inhibitory effect of licochalcone A on the *Plasmodium falciparum* respiratory chain. *Ann. NY Acad. Sci.* **1056**, 46–54
26. Ueno, H., Miyoshi, H., Ebisui, K., and Iwamura, H. (1994) Comparison of the inhibitory action of natural rotenone and its stereoisomers with various NADH-ubiquinone reductases. *Eur. J. Biochem.* **225**, 411–417
27. Tushurashvili, P.R., Gavrikova, E.V., Ledenev, A.N., and Vinogradov, A.D. (1985) Studies on the succinate dehydrogenating system. Isolation and properties of the mitochondrial succinate-ubiquinone reductase. *Biochim. Biophys. Acta* **809**, 145–159
28. Miyadera, H., Shiomi, K., Ui, H., Yamaguchi, Y., Masuma, R., Tomoda, H., Miyoshi, H., Osanai, A., Kita, K., and Omura, S. (2003) Atpenins, potent and specific inhibitors of mitochondrial complex II (succinate-ubiquinone oxidoreductase). *Proc. Natl Acad. Sci. USA* **100**, 473–477
29. Suraveratum, N., Krungkrai, S.R., Leangaramgul, P., Prapunwattana, P., and Krungkrai, J. (2000) Purification and characterization of *Plasmodium falciparum* succinate dehydrogenase. *Mol. Biochem. Parasitol.* **105**, 215–222
30. Yankovskaya, V., Horsefield, R., Tornroth, S., Luna-Chavez, C., Miyoshi, H., Leger, C., Byrne, B., Cecchini, G., and Iwata, S. (2003) Architecture of succinate dehydrogenase and reactive oxygen species generation. *Science* **299**, 700–704
31. Sun, F., Huo, X., Zhai, Y., Wang, A., Xu, J., Su, D., Bartlam, M., and Rao, Z. (2005) Crystal structure of mitochondrial respiratory membrane protein complex II. *Cell* **121**, 1043–1057
32. Huang, L.S., Sun, G., Cobessi, D., Wang, A.C., Shen, J.T., Tung, E.Y., Anderson, V.E., and Berry, E.A. (2006) 3-Nitropropionic acid is a suicide inhibitor of mitochondrial respiration that, upon oxidation by Complex II, forms a covalent adduct with a catalytic base arginine in the active site of the enzyme. *J. Biol. Chem.* **281**, 5965–5972
33. Schägger, H. and Pfeiffer, K. (2000) Supercomplexes in the respiratory chains of yeast and mammalian mitochondria. *EMBO J.* **19**, 1777–1783
34. Kerscher, S.J. (2000) Diversity and origin of alternative NADH:ubiquinone oxidoreductase. *Biochim. Biophys. Acta* **1459**, 274–283
35. De Vries, S. and Grivell, L.A. (1988) Purification and characterization of a rotenone-insensitive NADH:Q_6 oxidoreductase from mitochondria of *Saccharomyces cerevisiae*. *Eur. J. Biochem.* **176**, 377–341
36. Björklöf, K., Zickermann, V., and Finel, M. (2000) Purifiction of the 45 kDa, membrane bound NADH dehydrogenase of *Escherichia coli* (NDH-2) and analysis of its interaction with ubiquinone analogs. *FEBS Lett.* **467**, 105–110
37. Kerscher, S.J., Okun, J.G., and Brandt, U. (1999) A single external enzyme confers alternative NADH:ubiquinone oxidoreductase activity in *Yarrowia lipolytica*. *J. Cell Sci.* **112**, 2347–2354
38. Rasmusson, A.G., Fredlund, K.M., and Møller, I.M. (1993) Purification of a rotenone-insensitive NAD(P)H dehydrogenase from the inner surface of red beetroot mitochondria. *Biochim. Biophys. Acta* **1141**, 107–110
39. Luethy, M.H., Thelen, J.J., Knudten, A.F., and Elthon, T.E. (1995) Purification, characterization, and submitochondrial localization of a 58-kilodalton NAD(P)H dehydrogenase. *Plant Physiol.* **107**, 443–450
40. Yamashita, T., Nakamaru-Ogiso, E., Miyoshi, H., Matsuo-Yagi, A., and Yagi, T. (2007) Roles of bound quinone in the single subunit NADH-quinone oxidoreductase (Ndi1) from *Saccharomyces cerevisiae*. *J. Biol. Chem.* **282**, 6012–6020
41. Miyoshi, H., Takegami, K., Sakamoto, K., Mogi, T., and Iwamura, H. (1999) Characterization of the ubiquinol oxidation sites in cytochromes *bo* and *bd* from *Escherichia coli* using aurachin C analogues. *J. Biochem.* **125**, 138–142
42. Yano, T., Li, L.-S., Weinstein, E., The, J.-S., and Rubin, H. (2006) Steady-state kinetics and inhibitory action of antitubercular phenothiazines on *Mycobacterium tuberculosis* type-II NADH-menaquinone oxidoreductase (NDH-2). *J. Biol. Chem.* **281**, 11456–11463
43. Roos, M.H. and Tielens, A.G.M. (1994) Differential expression of two succinate dehydrogenase subunit-B genes and a transition in energy metabolism during the development of the parasitic nematode *Haemonchus contortus*. *Mol. Biochem. Parasitol.* **66**, 273–281
44. Saruta, F., Kuramochi, T., Nakamura, K., Takamiya, S., Yu, Y., Aoki, T., Sekimizu, K., Kojima, S., and Kita, K. (1995) Stage-specific isoforms of complex II (succinate-ubiquinone oxidoreductase) in mitochondria from the parasitic nematode, *Ascaris suum*. *J. Biol. Chem.* **270**, 928–932
45. Morales, J., Mogi, T., and Kita, K. (2008) Divergence in structure of mitochondrial respiratory Complex II (succinate-ubiquinone reductase) revealed by protozoan enzymes. *Biochim. Biophys. Acta* **1777**, S94–S95
46. Oyedotun, K.S. and Lemire, B.D. (1999) The *Saccharomyces cerevisiae* succinate-ubiquinone oxidoreductase. Identification of Sdh3p amino acid residues involved in ubiquinone binding. *J. Biol. Chem.* **274**, 23956–23962
47. Krungkrai, J., Kanchanarithisak, R., Krungkrai, S.R., and Sunant Rochanakij, S. (2002) Mitochondrial NADH dehydrogenase from *Plasmodium falciparum* and *Plasmodium berghei*. *Exp. Parasitol.* **100**, 54–61
48. Vaidya, A.B., Painter, H.J., Morrisey, J.M., and Mather, M.W. (2008) The validity of mitochondrial dehydrogenases as antimalarial drug targets. *Trends Parasitol.* **24**, 8–9
49. Saleh, A., Friesen, J., Baumeister, S., Gross, G., and Bohne, W. (2007) Growth inhibition of *Toxoplasma gondii* and *Plasmodium falciparum* by nanomolar concentrations of 1-hydroxy-2-dodecyl-4(1*H*)quinolone, a high-affinity inhibitor of alternative (type II) NADH dehydrogenases. *Antimicrob. Agents Chemother.* **51**, 1217–1222
50. Eschemann, A., Galkin, A., Oettmeier, W., Brandt, U., and Kerscher, S. (2005) HDQ (1-hydroxy-2-dodecyl-4(1*H*)quinolone), a high affinity inhibitor for mitochondrial

alternative NADH dehydrogenase: evidence for a ping-pong mechanism. *J. Biol. Chem.* **280**, 3138–3142

51. Speijer, D., Breek, C.K., Muijsers, A.O., Hartog, A.F., Berden, J.A., Albracht, S.P., Samyn, B., van Beeumen, J., and Benne, R. (1997) Characterization of the respiratory chain from cultured *Crithidia fasciculate*. *Mol. Biochem. Parasitol.* **85**, 171–186
52. Nelson, R.E., Aphasizheva, I., Falick, A.M., Nebohacova, M., and Simpson, L. (2004) The I-complex in *Leishmania tarentolae* is an uniquely-structured F_1-ATPase. *Mol. Biochem. Parasitol.* **135**, 221–224
53. Minagawa, N., Yabu, Y., Kita, K., Nagai, K., Ohta, N., Meguro, K., Sakajo, S., and Yoshimoto, A. (1997) An antibiotic, ascofuranone, specifically inhibits respiration and in vitro growth of long slender bloodstream forms of *Trypanosoma brucei brucei*. *Mol. Biochem. Parasitol* **84**, 271–280
54. Saimoto, H., Shigemasa, Y., Kita, K., Yabu, Y., Hosokawa, T., and Yamamoto, M. (2007) Novel phenol derivatives and antitrypanosoma preventive/therapeutic agent comprising the same as active ingredient. U.S. Patent 20070208078

RESEARCH LETTER

Identification of new inhibitors for alternative NADH dehydrogenase (NDH-II)

Tatsushi Mogi[1], Kazunobu Matsushita[2], Yoshiro Murase[3], Kenji Kawahara[1], Hideto Miyoshi[4], Hideaki Ui[5], Kazuro Shiomi[5], Satoshi Ōmura[5] & Kiyoshi Kita[1]

[1]Department of Biomedical Chemistry, Graduate School of Medicine, The University of Tokyo, Tokyo, Japan; [2]Department of Biological Chemistry, Faculty of Agriculture, Yamaguchi University, Yamaguchi, Japan; [3]Mycobacterium Reference Center, The Research Institute of Tuberculosis, Antituberculosis Association, Tokyo, Japan; [4]Division of Applied Life Sciences, Graduate School of Agriculture, Kyoto University, Kyoto, Japan; and [5]Kitasato Institute for Life Sciences and Graduate School of Infection Control Sciences, Kitasato University, Tokyo, Japan

Correspondence: Tatsushi Mogi, Department of Biomedical Chemistry, Graduate School of Medicine, The University of Tokyo, Bunkyo-ku, Tokyo 113-0033, Japan. Tel.: +81 3 5841 8202; fax: +81 3 5841 3444; e-mail: tmogi@m.u-tokyo.ac.jp

Received 7 October 2008; accepted 6 November 2008.
First published online 8 December 2008.

DOI:10.1111/j.1574-6968.2008.01451.x

Editor: Atsushi Yokota

Keywords
acetic acid bacteria; respiratory chain; NADH dehydrogenase; inhibitor; antibiotics.

Abstract

In bacterial membranes and plant, fungus and protist mitochondria, NADH dehydrogenase (NDH-II) serves as an alternative NADH : quinone reductase, a non-proton-pumping single-subunit enzyme bound to the membrane surface. Because NDH-II is absent in mammalian mitochondria, it is a promising target for new antibiotics. However, inhibitors for NDH-II are rare and unspecific. Taking advantage of the simple organization of the respiratory chain in *Gluconobacter oxydans*, we carried out screening of natural compounds and identified scopafungin and gramicidin S as inhibitors for *G. oxydans* NDH-II. Further, we examined their effects on *Mycobacterium smegmatis* and *Plasmodium yoelii* NDH-II as model pathogen enzymes.

Introduction

Obligate aerobe *Gluconobacter* is a genus of acetic acid bacteria that can oxidize a broad range of sugars, sugar alcohols and sugar acids. Low biomass yield and the rapid and incomplete oxidation of carbon sources (oxidative fermentation), which take place in the periplasm and is accompanied by the accumulation of products into the culture medium, make them suitable for industrial applications for bioconversion to obtain a variety of valuable products (Deppenmeier *et al.*, 2002; Adachi *et al.*, 2007). Key oxidation processes are catalyzed by dehydrogenases bound to the outer surface of the cytoplasmic membrane, and linked to the generation of proton-motive force (Matsushita *et al.*, 1994).

The recently released complete genome of *Gluconobacter oxydans* American Type Culture Collection 621H indicates that the respiratory chain lacks Complex I (NADH : quinone reductase, NDH-I), Complex II (succinate : quinone reductase) and Complex IV (cytochrome *c* oxidase) (Prust *et al.*, 2005). Genes encoding putative Complex III (quinol : cytochrome *c* reductase) and cytochrome *c* have been identified, but their functions are unclear because of the absence of cytochrome *c* oxidase. NADH produced in the cytoplasm is reoxidized by a single-subunit NADH dehydrogenase (NDH-II), a key enzyme for the regeneration of an oxidized form of NAD. NDH-II is bound peripherally to the inner surface of the cytoplasmic membrane and does not pump proton. Quinols generated by membrane-bound dehydrogenases are directly oxidized by cytochrome bo_3 oxidase (Matsushita *et al.*, 1987) and/or cyanide-insensitive oxidase (Ameyama *et al.*, 1987).

Taking advantage of the simple organization of the *Gluconobacter* respiratory chain (Matsushita *et al.*, 1994), here, we identified new inhibitors for NDH-II, which has been shown to be crucial for the adaptation of *Mycobacterium tuberculosis* (Shi *et al.*, 2005) and malaria parasite *Plasmodium* spp. (Fisher *et al.*, 2007) to host environments. From the screening of natural antibiotics in the Kitasato Institute for Life Sciences Chemical Library (Ui *et al.*, 2007),

we found the inhibitory activity of 36-membered ring macrolide scopafungin (Johnson & Dietz, 1971) and cyclic decapeptide gramicidin S (GS) (Izumiya *et al.*, 1979) (Fig. 1) for the *G. oxydans* NDH-II, and we examined their inhibitory mechanism and effects on *Mycobacterium smegmatis* and *Plasmodium yoelii* NDH-II.

Materials and methods

Preparation of bacterial membrane vesicles

Gluconobacter oxydans NBRC3172 (formerly *G. suboxydans* IFO12528) was grown aerobically in complex media containing 20 g of sodium D-gluconate, 5 g of D-glucose, 3 g of glycerol, 3 g of yeast extract and 2 g of polypepton (Nihon Pharmaceutical Co.) per 1 L using a 50-L jar fermentor at 30 °C. Cells were harvested at the late-log phase, suspended in 10 mM potassium phosphate (pH 6.0) and disrupted with a Rannie high-pressure laboratory homogenizer (model Mini-Lab, type 8.30H, Wilimington, MA). After centrifugation, to remove intact cells, the supernatant was centrifuged at 86 000 *g* for 60 min and precipitated membranes were suspended in 50 mM Tris-HCl (pH 7.4) containing 10% sucrose and 3 mM EDTA. *Mycobacterium smegmatis* mc^2155 was grown aerobically at 37 °C, and membrane vesicles were prepared from the stationary-phase cells (Kana *et al.*, 2001).

Preparation of malaria parasite mitochondria

Rodent malaria *P. yoelii* strain 17XL was injected intraperitoneally into 8-week-old female BALB/c mice, and parasite mitochondria were prepared as in Takashima *et al.* (2001). Rat liver mitochondria were prepared as in Johnson & Lardy (1967).

Enzyme assay

NADH : ubiquinone-1 (Q_1) reductase (NQR) activity of the membranes was measured at 25 °C in 100 mM Tris-HCl (pH 7.4) containing 10% sucrose, 0.02% Tween 20 (Calbiochem), 10 mM KCN and 100 μM Q_1 with a V-660 double monochromatic spectrophotometer (JASCO, Tokyo, Japan) (Mogi *et al.*, 2008), and reactions were initiated by addition of NADH ($\varepsilon_{340} = 6.3\ mM^{-1}\ cm^{-1}$, Roche) at a final concentration of 200 μM. Mitochondrial NQR and succinate : Q_1 reductase activities were determined in 50 mM potassium phosphate (pH 7.4) containing 1 mM $MgCl_2$, 0.02% Tween 20, 2 mM KCN and 100 μM Q_1 ($\varepsilon_{275} = 12.3\ mM^{-1}\ cm^{-1}$), and reactions were initiated by 200 μM NADH or 10 mM potassium succinate, respectively. NADH oxidase activity was measured in the absence of Q_1. Data analysis was carried out as in Mogi *et al.* (2008).

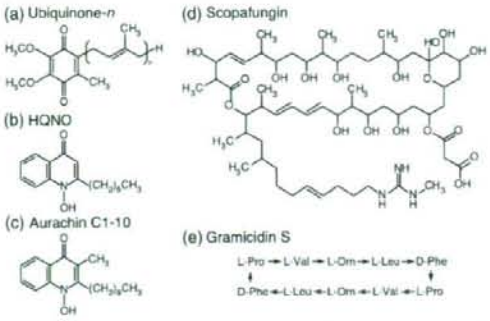

Fig. 1. Structures of ubiquinone, HQNO, aurachin C1–10, scopafungin and GS.

Materials

Synthesis of aurachin C 1-10 (Miyoshi *et al.*, 1999) was carried out as described previously. 2-Heptyl-4-hydroxyquinoline-*N*-oxide (HQNO) was obtained from Sigma.

Results and discussion

Screening of Kitasato Institute for Life Sciences Chemical Library

From the screening of a total of 304 microbial compounds (Ui *et al.*, 2007) at final concentrations of 5 μg mL^{-1} with *G. oxydans* membranes, we revealed the inhibitory activities of scopafungin (niphimycin; residual activity, 33%), GS (31%), polymixin B (51%), aculeacin A (63%), funiculosin (68%) and staurosporine (70%) on 0.2 mM NADH–0.1 mM Q_1 reductase activity of NDH-II.

Inhibitors for NDH-II are rare and mostly unspecific (Kerscher, 2000). Recently, quinolone derivatives [1-hydroxy-2-dodecyl-4(1*H*)quinolone, HQNO and aurachin C] were identified as potent inhibitors for the quinone reduction site of yeast NDH-II (Eschemann *et al.*, 2005; Yamashita *et al.*, 2007). We examined the effects of quinolone inhibitors on the *G. oxydans* NDH-II and found that HQNO and aurachin C 1-10 at 10 μM reduced the NQR activity of the *G. oxydans* membranes to 28% and 12%, respectively, of the control level. Because of the limitation in the availability of isolated natural compounds, we examined further effects of scopafungin and GS (Fig. 1), which are not structurally related to ubiquinone, but showed potent inhibitory activities on the *G. oxydans* NDH-II.

Determination of 50% inhibitory concentration (IC_{50}) values for NDH-II inhibitors

We examined the dependence of the NQR activity on the concentration of GS, scopafungin, HQNO and aurachin C 1-10 and determined their IC_{50} to be 1.2 ± 0.2, 6.2 ± 0.5,

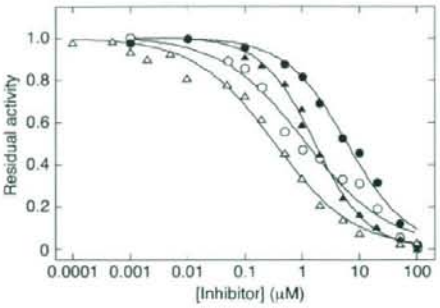

Fig. 2. Inhibition of *Gluconobacter oxydans* NDH-II by scopafungin, GS, HQNO and aurachin C 1-10. NQR activity of *G. oxydans* membranes (10 μg protein mL^{-1}) was determined in the presence of scopafungin (●), GS (○), HQNO (▲) or aurachin C1–10 (△). Data points were average values from duplicate assay. Control activity was 10.2 U mg^{-1} protein. IC_{50} values for GS, scopafungin, HQNO and aurachin C1–10 were estimated to be 1.2, 6.2, 1.7 and 0.34 μM, respectively.

1.7 ± 0.1 and 0.34 ± 0.04 μM, respectively (Fig. 2). The IC_{50} value for GS was < 3.5 μM for the *Escherichia coli bd*-type quinol oxidase (Mogi *et al.*, 2008), and the values for HQNO and aurachin C are comparable to 8 and 0.2 μM, respectively, of yeast *Saccharomyces cerevisiae* NDI1 (Yamashita *et al.*, 2007).

Kinetic analysis of inhibition of NADH-Q_1 reductase activity of NDH-II by scopafungin and GS

NADH-dependent NQR activity showed simple Michaelis–Menten kinetics with an apparent K_m value of 157 μM for NADH (at 0.2 mM Q_1) (Fig. 3). The K_m value for NADH was higher than those reported for yeast *Yarrowia lipolytica* NDE (15 μM) (Kerscher *et al.*, 1999), yeast *S. cerevisiae* NDI1 (31 μM) (de Vries & Grivell, 1988), human malaria *Plasmodium falciparum* NDH-II (17 μM) (Biagini *et al.*, 2006) and *E. coli* Ndh (34 μM) (Björklöf *et al.*, 2000). Q_1-dependent NQR activity followed Michaelis–Menten kinetics with an apparent K_m value of 16.2 ± 0.7 μM (Q_1) (Fig. 4), which is similar to 16 μM (Q_1) in *P. falciparum* (Biagini *et al.*, 2006), 5.9 μM (Q_1) in *E. coli* (Björklöf *et al.*, 2000), 6.4 μM (Q_2) in *M. tuberculosis* (Kana *et al.*, 2001) and 7 μM (decyl benzoquinone) in *Y. lipolytica* (Eschemann *et al.*, 2005).

Macrolide scopafungin and cyclic decapeptide GS (Fig. 1) are structurally unrelated to both NADH and ubiquinone, and serve as noncompetitive inhibitors ($K_i = 5.5$ and 1.4 μM, respectively) for the NADH-binding site of NDH-II (Fig. 3). Unexpectedly, scopafungin and GS were found to be a mixed-type inhibitor and a competitive inhibitor for the quinone-binding site, respectively (Fig. 4). These results

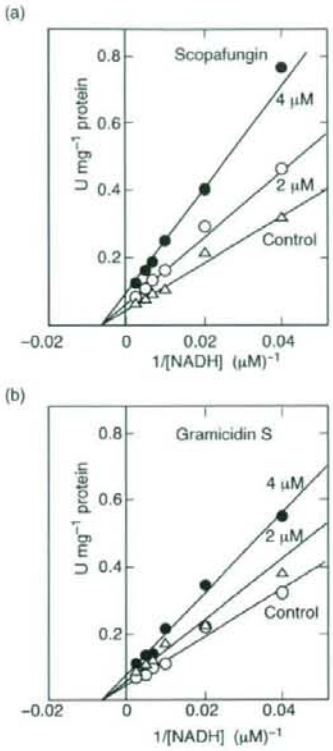

Fig. 3. Kinetic analysis of effects of scopafungin and GS on the NADH-dependent NQR activity of *Gluconobacter oxydans* NDH-II. (a) Noncompetitive inhibition by scopafungin. Apparent V_{max} values were estimated to be 19.3 (control), 17.2 (2 μM scopafungin) and 11.9 (4 μM scopafungin) U mg^{-1} protein at $K_m = 157$ μM. (b) Noncompetitive inhibition by GS. Apparent V_{max} values were determined to be 21.9 (control), 16.5 (2 μM GS) and 13.2 (4 μM GS) U mg^{-1} protein at $K_m = 157$ μM.

indicate that both compounds bind to a hydrophobic binding pocket on NDH-II molecule, which is closer to the quinone reduction site.

Effects of scopafungin and GS on *M. smegmatis* and *P. yoelii* NDH-II

Macrolide antibiotics are known to be more active against Gram-positive bacteria and fungi (Izumiya *et al.*, 1979), but targets remain to be determined while GS is active against Gram-positive and Gram-negative bacteria and several pathogenic fungi (Kondejewski *et al.*, 1996). The primary mode of the action of GS is generally assumed to perturb lipid packing, resulting in the destruction of the membrane integrity and enhancement of the permeability of the lipid bilayer (Prenner *et al.*, 1997). Very recently, we found that

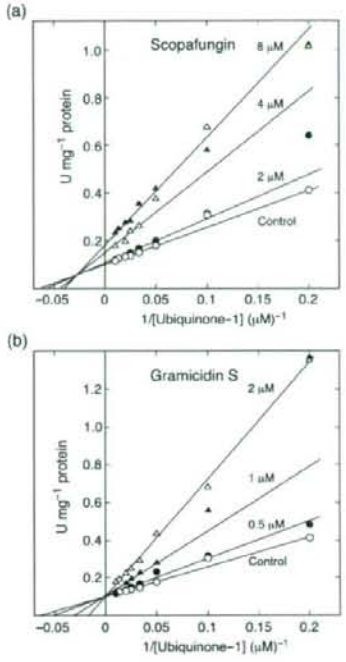

Fig. 4. Kinetic analysis of effects of scopafungin and GS on the Q_1-dependent NQR activity of *Gluconobacter oxydans* NDH-II. (a) Mixed-type inhibition by scopafungin. Apparent K_m (μM) and V_{max} (U mg^{-1} protein) values were estimated to be 15.5 and 9.6 (control), 17.4 and 9.0 (2 μM scopafungin), 22.4 and 6.5 (4 μM scopafungin) and 24.9 and 5.3 (8 μM scopafungin). (b) Competitive inhibition by GS. The apparent K_m values were determined to be 16.9 (control), 21.7 (0.5 μM GS), 37.5 (1 μM GS) and 68.3 (2 μM GS) μM at V_{max} = 10.1 U mg^{-1} protein.

Table 1. Effects of GS and scopafungin on the rat liver mitochondrial respiratory enzymes

	Relative residual activity (%)	
Enzyme activity	10 μM GS	10 μM scopafungin
NADH : Q_1 reductase (Complex I)	107	89
Succinate : Q_1 reductase (Complex II)	90	82
NADH oxidase (Complexes I+III+IV)	35	84

Control activities were 154 (NADH : Q_1 reductase), 247 (succinate : Q_1 reductase) and 102 (NADH oxidase) mU mg^{-1} protein.

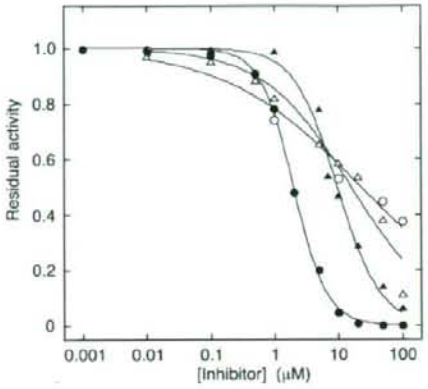

Fig. 5. Inhibition of *Mycobacterium smegmatis* and *Plasmodium yoelii* NDH-II by GS and scopafungin. Control activities of *M. smegmatis* membranes and *P. yoelii* mitochondria were 1.1 and 0.071 U mg^{-1} protein, respectively. The IC_{50} values for GS were estimated to be 2.0 (*M. smegmatis*, ●) and 23 (*P. yoelii*, ○) μM and those for scopafungin were 9.8 (*M. smegmatis*, ▲) and 16 (*P. yoelii*, △) μM.

GS can directly inhibit the *E. coli bd*-type quinol oxidase in a mixed-type manner (Mogi *et al.*, 2008). From the screening of the Kitasato Institute for Life Sciences Chemical Library with *G. oxydans* membranes, here, we identified scopafungin and GS as new inhibitors for NDH-II.

NDH-II is a promising target of new antibiotics because of the absence of NDH-II in mammalian mitochondria. The antiplasmodial activities of NDH-II inhibitors, HQNO (IC_{50} = 3.5 μM) (Fry *et al.*, 1990) and 1-hydroxy-2-dodecyl-4(1H) quinolone (IC_{50} = 14 nM) (Saleh *et al.*, 2007), have been reported previously. Thus, we examined the effects of scopafungin and GS on the NQR activity of *M. smegmatis* and rodent malaria *P. yoelii* NDH-II. At 10 μM, scopafungin showed minor effects on rat liver mitochondrial Complex I, Complex II and Complex III *plus* IV, while GS reduced NADH oxidase activity to 35% of the control by inhibiting the Complex III *plus* IV activity (Table 1). Although the IC_{50} values of scopafungin and GS for rodent malaria NDH-II were rather high (16.1 ± 3.0 and 23.0 ± 7.1 μM, respectively), both scopafungin and GS inhibited *M. smegmatis* NDH-II with IC_{50} values of 9.8 ± 0.7 and 2.0 ± 0.1 μM, respectively (Fig. 5), which are better than 12 μM of trifluoperazine for *M. tuberculosis* NDH-II (Yano *et al.*, 2006). Because scopafungin did not show severe effects on mammalian respiratory enzymes, it is a candidate for antimycobacterial agents. Here, we showed that the Kitasato Institute for Life Sciences Chemical Library (Ui *et al.*, 2007) was a powerful source for new potent antibiotics targeting to respiratory enzymes. For the identification of potential candidates, screening with recombinant NDH-IIs is currently underway in our laboratory.

Acknowledgements

This study was supported by a grant-in-aid for scientific research (20570124 to T.M.), scientific research on Priority Areas (18073004 to K.K.) and Creative Scientific Research (18GS0314 to K.K.) from the Japanese Ministry of Education, Science, Culture, Sports, and Technology.

References

Adachi O, Ano Y, Toyama H & Matsushita K (2007) Biooxidation with PQQ- and FAD-dependent dehydrogenases. *Modern Biooxidation, Enzymes, Reactions and Applications* (Schmid RD & Urlacher VB, eds), pp. 1–41. Wiley-VCH, Weinheim.

Ameyama M, Matsushita K, Shinagawa E & Adachi O (1987) Sugar-oxidizing respiratory chain of *Gluconobacter suboxydans*. Evidence for a branched respiratory chain and characterization of respiratory chain-linked cytochromes. *Agr Biol Chem* **51**: 2943–2950.

Biagini GA, Viriyavejakul P, O'Neill PM, Bray PG & Ward SA (2006) Functional characterization and target validation of alternative Complex I of *Plasmodium falciparum* mitochondria. *Antimicrob Agents Ch* **50**: 1841–1851.

Björklöf K, Zickermann V & Finel M (2000) Purifiction of the 45 kDa, membrane bound NADH dehydrogenase of *Escherichia coli* (NDH-2) and analysis of its interaction with ubiquinone analogs. *FEBS Lett* **467**: 105–110.

Deppenmeier U, Hoffmeister M & Prust C (2002) Biochemistry and biotechnological applications of *Gluconobacter* strains. *Appl Microbiol Biot* **60**: 233–242.

De Vries S & Grivell LA (1988) Purification and characterization of a rotenone-insensitive NADH : Q_6 oxidoreductase from mitochondria of *Saccharomyces cerevisiae*. *Eur J Biochem* **176**: 377–341.

Eschemann A, Galkin A, Oettmeier W, Brandt U & Kerscher S (2005) HDQ (1-hydroxy-2-dodecyl-4(1*H*)quinolone), a high affinity inhibitor for mitochondrial alternative NADH dehydrogenase: evidence for a ping-pong mechanism. *J Biol Chem* **280**: 3138–3142.

Fisher N, Bray PG, Ward SA & Biagini GA (2007) The malaria parasite type II NADH : quinone oxidoreductase: an alternative enzyme for an alternative lifestyle. *Trends Parasitol* **23**: 305–310.

Fry M, Webb E & Pudney M (1990) Effect of mitochondrial inhibitors on adenosine triphosphate levels in *Plasmodium falciparum*. *Comp Biochem Physiol* **B96**: 775–782.

Izumiya N, Kato T, Aoyaga H, Waki M & Kondo M (1979) *Synthetic Aspects of Biologically Active Cyclic Peptides: Gramicidin S and Tyrocidines*. Halsted Press, New York.

Johnson D & Lardy H (1967) Isolation of liver or kidney mitochondria. *Methods in Enzymology, Vol. 10* (Estabrook RW & Pullman ME, eds), pp. 94–96. Academic Press, New York.

Johnson LE & Dietz A (1971) Scopafungin, a crystalline antibiotic produced by *Streptomyces hygroscopicus* var. *enhygrus* var. *nova*. *Appl Microbiol* **22**: 303–308.

Kana BD, Weinstein EA, Avarbock D, Dawes SS, Rubin H & Mizrahi V (2001) Characterization of the *cydAB*-encoded cytochrome *bd* oxidase from *Mycobacterium smegmatis*. *J Bacteriol* **183**: 7076–7086.

Kerscher SJ (2000) Diversity and origin of alternative NADH : ubiquinone oxidoreductase. *Biochim Biophys Acta* **1459**: 274–283.

Kerscher SJ, Okun JG & Brandt U (1999) A single external enzyme confers alternative NADH : ubiquinone oxidoreductase activity in *Yarrowia lipolytica*. *J Cell Sci* **112**: 2347–2354.

Kondejewski LH, Farmer SW, Wishart D, Kay CM, Hancock REW & Hodges RS (1996) Modulation of structure and antibacterial and hemolytic activity by ring size in cyclic gramicidin S analogs. *J Biol Chem* **271**: 25261–25268.

Matsushita K, Shinagawa E, Adachi O & Ameyama M (1987) Purification and characterization of cytochrome *o*-type oxidase from *Gluconobacter suboxydans*. *Biochim Biophys Acta* **894**: 304–312.

Matsushita K, Toyama H & Adachi O (1994) Respiratory chains and bioenergetics of acetic acid bacteria. *Advances in Microbial Physiology, Vol. 36* (Rose AH & Tempest DW, eds), pp. 247–301. Academic Press Ltd, London.

Miyoshi H, Takegami K, Sakamoto K, Mogi T & Iwamura H (1999) Characterization of the ubiquinol oxidation sites in cytochromes *bo* and *bd* from *Escherichia coli* using aurachin C analogues. *J Biochem* **125**: 138–142.

Mogi T, Ui H, Shiomi K, Ômura S & Kit K (2008) Gramicidin S identified as a potent inhibitor for cytochrome *bd*-type quinol oxidase. *FEBS Lett* **582**: 2299–2302.

Prenner EJ, Lewis RNAH, Newman KC, Gruner SM, Kondejewski LH, Hodges RS & McElhaney RN (1997) Nonlamellar phases induced by the interaction of gramicidin S with lipid bilayers. A possible relationship to membrane disrupting activity. *Biochemistry* **36**: 7906–7916.

Prust C, Hoffmeister M, Liesegang H, Wiezer A, Fricke WF, Ehrenreich A, Gottschalk G & Deppenmeier U (2005) Complete genome sequence of the acetic acid bacterium *Gluconobacter oxydans*. *Nat Biotechnol* **23**: 195–200.

Saleh A, Friesen J, Baumeister S, Gross G & Bohne W (2007) Growth inhibition of *Toxoplasma gondii* and *Plasmodium falciparum* by nanomolar concentrations of 1-hydroxy-2-dodecyl-4(1*H*)quinolone, a high-affinity inhibitor of alternative (type II) NADH dehydrogenases. *Antimicrob Agents Ch* **51**: 1217–1222.

Shi L, Sohaskey CD, Kana BD, Dawes S, North RJ, Mizrahi V & Gennaro ML (2005) Changes in energy metabolism of *Mycobacterium tuberculosis* in mouse lung and under *in vitro* conditions affecting aerobic respiration. *P Natl Acad Sci USA* **102**: 15629–15634.

Takashima E, Takamiya S, Takeo S, Mi-ichia F, Amino H & Kita K (2001) Isolation of mitochondria from *Plasmodium falciparum* showing dihydroorotate dependent respiration. *Parasitol Int* **50**: 273–278.

Ui H, Ishiyama A, Sekiguchi H, Namatame M, Nishihara A, Takahashi A, Shiomi K, Otoguro K & Ômura S (2007) Selective and potent *in vitro* antimalarial activities found in four microbial metabolites. *J Antibiot* **60**: 220–222.

Yamashita T, Nakamaru-Ogiso E, Miyoshi H, Matsuo-Yagi A & Yagi T (2007) Roles of bound quinone in the single subunit NADH–quinone oxidoreductase (Ndi1) from *Saccharomyces cerevisiae*. *J Biol Chem* **282**: 6012–6020.

Yano T, Li L-S, Weinstein E, The J-S & Rubin H (2006) Steady-state kinetics and inhibitory action of antitubercular phenothiazines on *Mycobacterium tuberculosis* type-II NADH-menaquinone oxidoreductase (NDH-2). *J Biol Chem* **281**: 11456–11463.

THE JOURNAL OF BIOLOGICAL CHEMISTRY VOL. 284, NO. 11, pp. 7255–7263, March 13, 2009

Novel Mitochondrial Complex II Isolated from *Trypanosoma cruzi* Is Composed of 12 Peptides Including a Heterodimeric Ip Subunit*[S]

Received for publication, August 26, 2008, and in revised form, January 2, 2009 Published, JBC Papers in Press, January 2, 2009, DOI 10.1074/jbc.M806623200

Jorge Morales[‡1], Tatsushi Mogi[‡2], Shigeru Mineki[§], Eizo Takashima[‡3], Reiko Mineki[¶], Hiroko Hirawake[‡], Kimitoshi Sakamoto[‡], Satoshi Omura[‖], and Kiyoshi Kita[‡4]

From the [‡]Department of Biomedical Chemistry, Graduate School of Medicine, the University of Tokyo, Hongo, Bunkyo-ku, Tokyo 113-0033, the [§]Department of Applied Biological Science, Faculty of Science and Technology, Tokyo University of Science, Noda, Chiba 278-8510, the [¶]Division of Proteomics and BioMolecular Science, Juntendo University Graduate School of Medicine, Hongo, Bunkyo-ku, Tokyo 113-8421, and the [‖]Kitasato Institute for Life Sciences and Graduate School of Infection Control Sciences, Kitasato University, Minato-ku, Tokyo 108-8641, Japan

Mitochondrial respiratory enzymes play a central role in energy production in aerobic organisms. They differentiated from the α-proteobacteria-derived ancestors by adding non-catalytic subunits. An exception is Complex II (succinate: ubiquinone reductase), which is composed of four α-proteobacteria-derived catalytic subunits (SDH1–SDH4). Complex II often plays a pivotal role in adaptation of parasites in host organisms and would be a potential target for new drugs. We purified Complex II from the parasitic protist *Trypanosoma cruzi* and obtained the unexpected result that it consists of six hydrophilic (SDH1, $SDH2_N$, $SDH2_C$, and SDH5–SDH7) and six hydrophobic (SDH3, SDH4, and SDH8–SDH11) nucleus-encoded subunits. Orthologous genes for each subunit were identified in *Trypanosoma brucei* and *Leishmania major*. Notably, the iron-sulfur subunit was heterodimeric; $SDH2_N$ and $SDH2_C$ contain the plant-type ferredoxin domain in the N-terminal half and the bacterial ferredoxin domain in the C-terminal half, respectively. Catalytic subunits (SDH1, $SDH2_N$ plus $SDH2_C$, SDH3, and SDH4) contain all key residues for binding of dicarboxylates and quinones, but the enzyme showed the lower affinity for both substrates and inhibitors than mammalian enzymes. In addition, the enzyme binds protoheme IX, but SDH3 lacks a ligand histidine. These unusual features are unique in the Trypanosomatida and make their Complex II a target for new chemotherapeutic agents.

The parasitic protist *Trypanosoma cruzi* is the etiological agent of Chagas disease, a public health threat in Central and South America. These parasites are normally transmitted by reduviid bugs via the vector feces after a bug bite and also via transfusion of infected blood. About 16–18 million people are infected, and 100 million are at risk, but there are no definitive chemotherapeutic treatments available (1). Despite having potential pathways for oxidative phosphorylation (2), all trypanosomatids (*Trypanosoma* and *Leishmania* species) analyzed so far are characterized by incomplete oxidation of glucose with secretion of end products, such as succinate, alanine, ethanol, acetate, pyruvate, and glycerol (3, 4) (Fig. 1). Major routes for formation of succinate in *Trypanosoma brucei* are via NADH-dependent fumarate reductase in glycosomes and mitochondria (5, 6). In trypanosomatid mitochondria, the Krebs cycle is inefficient, and pyruvate is principally converted to acetate via acetate:succinate CoA transferase (7). A part of the Krebs cycle operates the utilization of histidine in the insect stage of *T. cruzi* (8).

Mitochondrial Complex II (succinate:quinone reductase (SQR)[5] and succinate dehydrogenase (SDH)) serves as a membrane-bound Krebs cycle enzyme and often plays a pivotal role in adaptation of parasites to environments in their host (9, 10). In general, Complex II consists of four subunits (11). A flavoprotein subunit (SDH1, Fp) and an iron-sulfur subunit (SDH2, Ip) form a soluble heterodimer, which then binds to a membrane anchor heterodimer, SDH3 (CybL) and SDH4 (CybS). SDH1 contains a covalently bound FAD and catalyzes the oxidation of succinate to fumarate. SDH2 transfers electrons to ubiquinone via the [2Fe-2S] cluster in the N-terminal plant-type ferredoxin domain (Ip_N) and the [4Fe-4S] and [3Fe-4S] clusters in the C-terminal bacterial ferredoxin domain (Ip_C). Ubiquinone is bound and reduced in a pocket provided by SDH2, SDH3, and SDH4 (12–14). SDH3 and SDH4 contain three transmembrane helices and coordinate protoheme IX via histidine in the second helices of each subunit (11–14).

* This work was supported in part by Grant-in-aid for Scientific Research 20570124 (to T. M.), Creative Scientific Research Grant 18GS0314 (to K. K.), Grant-in-aid for Scientific Research on Priority Areas 18073004 (to K. K.) from the Japanese Society for the Promotion of Science, and Targeted Proteins Research Program (to K. K.) from the Japanese Ministry of Education, Science, Culture, Sports and Technology (MEXT). The costs of publication of this article were defrayed in part by the payment of page charges. This article must therefore be hereby marked "*advertisement*" in accordance with 18 U.S.C. Section 1734 solely to indicate this fact.

[S] The on-line version of this article (available at http://www.jbc.org) contains supplemental Table S1.

[1] Supported by a Japanese Government scholarship from Ministry of Education, Science, Culture, Sports and Technology.

[2] To whom correspondence may be addressed. Tel.: 81-3-5841-3526; Fax: 81-3-5841-3444; E-mail: tmogi@m.u-tokyo.ac.jp.

[3] Present address: Dept. of Microbiology, School of Life Dentistry at Tokyo, Nippon Dental University, Tokyo 102-8159, Japan.

[4] To whom correspondence may be addressed. Tel.: 81-3-5841-3526; Fax: 81-3-5841-3444; E-mail: kitak@m.u-tokyo.ac.jp.

[5] The abbreviations used are: SQR, succinate:quinone reductase; hrCNE, high resolution clear native electrophoresis; IC_{50}, the 50% inhibitory concentration; Ip_N, the N-terminal plant-type ferredoxin domain; Ip_C, the C-terminal bacterial ferredoxin domain; DCIP, 2,4-dichlorophenolindophenol; SML, sucrose monolaurate; Tricine, *N*-[2-hydroxy-1,1-bis(hydroxymethyl)ethyl]-glycine; MOPS, 3-(*N*-morpholino)propanesulfonic acid; Q_n, ubiquinone-*n*.

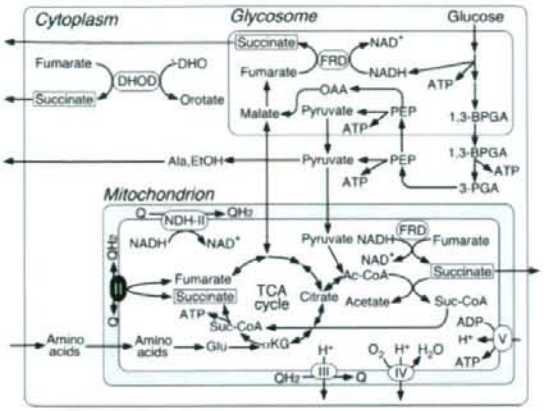

FIGURE 1. **Metabolic pathways in *T. cruzi*.** Incomplete oxidation of glucose takes place in glycosomes and mitochondria, and end products such as succinate, L-alanine, ethanol, and acetate are excreted from parasites (3, 4). Cytoplasmic dihydroorotate (*DHO*):fumarate reductase (*DHOD*) contributes succinate production (6).

TABLE 1
Purification of complex II from *T. cruzi* mitochondria

Step	Protein	Succinate:DCIP reductase	Yield	Purification
	mg	*units*	*units/mg*	%	*-fold*
Mitochondria	314	27	0.085	100	1.0
SML extract	141	22	0.16	83	1.9
Source 15Q	7.8	7.6	0.97	28	12
Superdex 200 (1st)	1.3	1.4	1.09	5.3	13
Superdex 200 (2nd)	0.15	0.43	2.87	1.6	34

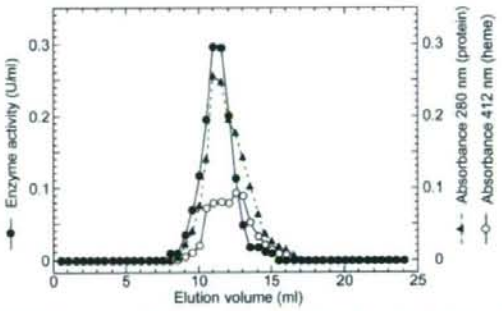

FIGURE 2. **Elution profile of *T. cruzi* Complex II on Superdex 200 chromatography.** Complex II fractions from the first gel filtration chromatography with a Superdex 200-pg column were concentrated and rechromatographed at the flow rate of 0.25 ml/min. Aliquots were collected every 0.5 ml. Elution profiles for proteins and cytochromes were monitored at 280 (▲) and 412 nm (○), respectively, and the enzyme activity (●) was measured as decylquinone-mediated succinate:DCIP reductase.

Parasitic nematodes adapted to hypoxic host environments often have modified respiratory chains. Many adult parasites perform fumarate respiration by expressing a stage-specific isoform of Complex II (9, 10). *Hemonchus contortus* uses an isoform for SDH2 (9), whereas *Ascaris suum* uses isoforms for SDH1 and SDH4 (10). To explore the adaptive strategy in a parasitic protist, we isolated mitochondria from axenic culture of *T. cruzi* epimastigotes and characterized the purified Complex II. Our results demonstrated for the first time that *T. cruzi* Complex II is an unusual supramolecular complex with a heterodimeric iron-sulfur subunit and seven novel noncatalytic subunits. Purified enzyme showed reduced binding affinities for both substrates and inhibitors. Because this novel structural organization is conserved in all trypanosomatids (2, 15, 16), parasite Complex II would be a potential target for the development of new chemotherapeutic agents for trypanosomiasis and leishmaniasis.

EXPERIMENTAL PROCEDURES

Preparation of Mitochondria—*T. cruzi* strain Tulahuhen was grown statically for 6–7 days at 26 °C in 300-cm^2 cell culture flasks (Falcon, BD Biosciences) containing 250 ml of the modified LIT medium (17), supplemented with 0.1% (w/v) glucose, 0.001% (w/v) hemin (Sigma), and 5% (v/v) fetal bovine serum (MP Biochemicals). Mitochondria were isolated from epimastigotes by the differential centrifugation method (18) with slight modifications. Parasites grown to $6-8 \times 10^7$ cells/ml were washed with buffer A (20 mM Tris-HCl, pH 7.2, 10 mM NaH_2PO_4, 1 mM sodium EDTA, 1 mM dithiothreitol, 0.225 M sucrose, 20 mM KCl, and 5 mM $MgCl_2$). Cells were disrupted by grinding with silicon carbide (Carborundum 440 mesh; Nacalai Tesque, Kyoto, Japan) in the presence of a minimum volume of buffer B (25 mM Tris-HCl, pH 7.6, 1 mM dithiothreitol, 1 mM sodium EDTA, 0.25 M sucrose, and EDTA-free Complete protease inhibitor mixture (Roche Applied Science)). The resultant cell paste was resuspended in buffer B and centrifuged at 500 × *g* for 5 min and 1000 × *g* for 15 min to remove silicon carbide and nuclear fraction, respectively. The mitochondrial fraction was recovered upon centrifugation of the last supernatant at 10,000 × *g* for 15 min, washed three times in buffer B, and resuspended to a protein concentration of ~30 mg/ml and kept at −80 °C until use.

Isolation of Complex II—All steps were carried out at 4 °C. Mitochondrial fraction (~300 mg of protein from 10 liters culture) was brought to 70 ml with buffer C (10 mM KP_i, pH 7.5), 1 mM sodium EDTA, 1 mM sodium malonate, EDTA-free Complete protease inhibitor mixture (Roche Applied Science) (2 tablets/50 ml), 1% (w/v) sucrose monolaurate SM-1200 (SML) (Mitsubishi-Kagaku Foods Co., Tokyo, Japan)). The mixture was stirred for 30 min and centrifuged at 200,000 × *g* for 1 h. The supernatant was loaded at 1 ml/min onto a Source 15 Q column (1.6 inner diameter × 10 cm; GE Healthcare), equilibrated with buffer C containing 0.1% SML. After washing with 5 volumes of the same buffer, proteins were eluted with a 200-ml linear gradient of NaCl from 0 to 150 mM at 2 ml/min. Active fractions were concentrated to ~250 μl by ultrafiltration with Amicon Ultra-4 (molecular weight cutoff 100,000, Millipore) and subjected to gel filtration FPLC with a Superdex 200-pg 10/300 GL column (1 cm inner diameter × 30 cm; GE Healthcare) at 0.25 ml/min in 20 mM MOPS-NaOH, pH 7.2, containing 1 mM sodium EDTA, 1 mM sodium malonate, 150 mM NaCl, and 0.1% SML. Peak fractions were rechromatographed as above, and purified enzyme was concentrated and stored at −80 °C until use.

Identification of Complex II Subunits—The purified enzyme was subjected to 12.5% SDS-PAGE, and subunits were transferred to an Immobilon-P membrane (Millipore), followed by

staining with Coomassie Brilliant Blue R-250 (19, 20). Five or ten N-terminal amino acid residues were determined with a Procise 494 HT (Applied Biosystems) or an Hp G1005A (Hewlett-Packard Co.) Protein Sequencing System at the Bio-Medical Research Center of Juntendo University or APRO Life Science Institute, Inc. (Tokushima, Japan). When the N terminus was blocked, protein bands were digested with trypsin, and internal peptide sequences were determined (20). Genes coded for Complex II subunits were identified with BLASTP in the *T. cruzi* genome data base (15).

Phase Partitioning of Mitochondrial Fraction with Triton X-114—Phase partitioning by Triton X-114 was performed as described previously (21) with a slight modification. A total of 2–3 mg of mitochondrial fraction was resuspended in 1 ml of Tris-HCl, pH 7.5, 150 mM NaCl, 1 mM EDTA, 2 mM sodium malonate, Complete protease inhibitors mixture (Roche Applied Science) (2 tablets/50 ml), protease inhibitors mixture for mammalian cell and tissue extracts (Sigma) (10 μl/ml), and 2% (v/v) Triton X-114. The mixture was incubated for 30 min on ice and kept at −30 °C overnight. After thawing, the insoluble material was removed by centrifugation at 4 °C, and the supernatant was incubated for 10 min at 37 °C and centrifuged at 2000 × *g* for 10 min to separate the aqueous and detergent-rich phases. The aqueous phase was brought to 2% (v/v) Triton X-114, whereas the detergent-rich fraction was brought to 1 ml with the above buffer. After incubation on ice for 10 min, samples were incubated at 37 °C for 10 min and phases separated as before. This wash step was repeated three times. Finally, the samples were dialyzed and concentrated by Amicon Ultra-4 (Millipore) in the presence of 50 mM imidazole, 50 mM NaCl, 6 mM aminocaproic acid, 0.05% (w/v) deoxycholate, and 0.1% (w/v) SML, pH 7, and kept at −80 °C until use.

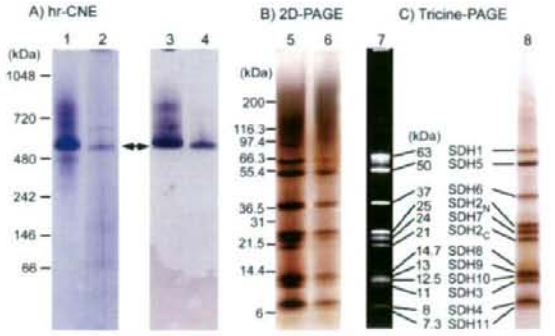

FIGURE 3. **Electrophoresis analysis of *T. cruzi* Complex II.** *A*, purified Complex II (2 μg; *lanes 1* and *3*) and the detergent-rich fraction from the phase partitioning by Triton X-114 of the mitochondrial fraction (60 μg; *lines 2* and *4*) were subjected to hrCNE. Proteins were stained by Coomassie Brilliant Blue (*left panel*), and Complex II was visualized by SDH activity staining (*right panel*). *B*, proteins of Complex II showing SDH activity in *A* were analyzed by 10–20% Tricine SDS-PAGE and visualized by silver stain (*lane 5*, pure complex; *lane 6*, detergent-rich fraction). *C* shows the subunit composition of the pure Complex II from *T. cruzi* stained by SYPRO ruby (*lane 7*) or silver stain (*lane 8*). Molecular weight standards used are NativeMark (Invitrogen, *lane 1*) and Mark 12 unstained standards (Invitrogen, *lanes 5* and *7*).

Enzyme Assay—Decylubiquinone-mediated succinate-2,4 dichlorophenolindophenol (DCIP) reductase activity was measured at 25 °C in 100 mM potassium phosphate, pH 7.4, containing 1 mM $MgCl_2$, 2 mM KCN, 0.1 mM antimycin A (Sigma), and 0.1% SML with 63 μM decylubiquinone (Sigma) *plus* 60 μM DCIP. After 2 min of incubation, reduction of DCIP (ϵ_{600} = 21 mM^{-1} cm^{-1}) was measured in the presence of 10 mM succinate. SQR activity was determined with 40 μM ubiquinone-2 (Q_2) (Sigma, ϵ_{278} = 12.3 mM^{-1} cm^{-1}). Kinetic analysis was done with KaleidaGraph version 4.0 (Synergy Software).

Miscellaneous—High resolution clear native electrophoresis (hrCNE) (22) was performed with 4–16% Novex gels (Invitrogen) using 0.02% dodecylmaltoside and 0.05% sodium deoxycholate for the cathode buffer additives, and the Complex II band was visualized by the activity staining (23) or Coomassie Brilliant Blue. Tricine-PAGE analysis was done with Novex 10–20% Tricine gels (Invitrogen), and proteins bands were sequentially stained by Sypro ruby (Invitrogen) and silver. During purification the succinate-decylubiquinone-DCIP reduc-

TABLE 2
Identification of genes encoding subunits for *T. cruzi* complex II

Subunit[a]	Sequence confirmed[b]	Accession number or RefSeq ID at NCBI (haplotype,[c] M_r)	Identity[d]	TM[e]
			%	
SDH1	Ser^{10}–Met^{19}	AB031741 (NE, 66,974), XP_809281 (E, 18,231)	59	0
SDH5	Ala^{10}–Leu^{19}	XP_818124 (NE, 53,831), XP_810172 (E, 20,788)	16	0
$SDH2_N$	Ser^{188}–Arg^{196}, Lys^{201}–Ile^{204}, Gly^{221}–Asn^{223}, Glu^{267}–Ile^{269}	XP_814994 (merged, 32,232)[f]	24 (37)	0
$SDH2_C$	Pro^{2}–Leu^{6}	XP_803796 (NE, 21,352), XP_806126 (E, 21,379)	25 (43)	0
SDH6a	Val^{19}–Val^{28}	XP_809065 (NA, 36,077), XP_812789 (NA, 36,035)	15	0
SDH6b	Val^{19}–Val^{28}	XP_813603 (NA, 36,133), XP_813645 (NA, 36,039)	14	0
SDH7	Ile^{26}–Leu^{35}	XP_813318 (NE, 28,218), XP_820239 (E, 28,202)	22	0
SDH3	Val^{2}–Phe^{11}	XP_809410 (NE, 12,176), XP_810064 (E, 12,204)	29	1
SDH4	Phe^{39}–Thr^{46}	XP_808211 (E, 13,957), XP_816430 (NE, 13,975)	27	2
SDH8	Gly^{5}–Met^{16}	XP_809192 (NE, 16,199), XP_817545 (E, 16,143)	ND[g]	2
SDH9	Ile^{10}–Pro^{19}	XP_807105 (merged, 15,736)	ND	1
SDH10	Pro^{25}–Val^{33}	XP_808894 (NE, 15,565), XP_808903 (E, 15,554)	ND	1
SDH11	Phe^{20}–Cys^{29}	XP_814088 (E, 10,346), XP_814509 (NE, 10,337)	ND	1

[a] Alleles were named as SDH3-1 (XP_809410) and SDH3-2 (XP_810064) in the order of the accession numbers, except for SDH5.
[b] These are N-terminal sequences except for $SDH2_N$ and SDH8, where the N-terminal residues were blocked.
[c] Homozygous alleles located in a merged assembly of Esmeraldo (E) and non-Esmeraldo (NE) homologous sequences whose different copies were merged genes during the genome assembly are indicated by "merged." Haplotypes for gene with more than two copies in the genome that does not belong to a merged region are not assigned (NA).
[d] Identity % to counterparts in human were as follows: SDH1 (D30648), SDH2 (P21912), SDH3 (Q99643), or SDH4 (O14521). In parentheses, the identity % of $SDH2_N$ and $SDH2_C$ that correspond to either Met^{1}–Pro^{155} (Ip_N domain) or Tyr^{156}–Val^{280} (Ip_C domain), respectively, of human SDH2 is shown. Identity % for truncated forms of SDH1 and SDH5 (SDH1-2 and SDH5-2) in the Esmeraldo haplotype was 66 and 20%, respectively.
[e] Transmembrane segments (TM) were estimated with TMHMM (52) and SOSUI (53).
[f] SDH2N from other trypanosomatids lack Met^{1} to Arg^{82} of $TcSDH2_N$.
[g] ND indicates not determined because these hydrophobic sequences are a highly divergent form of mammalian sequences.

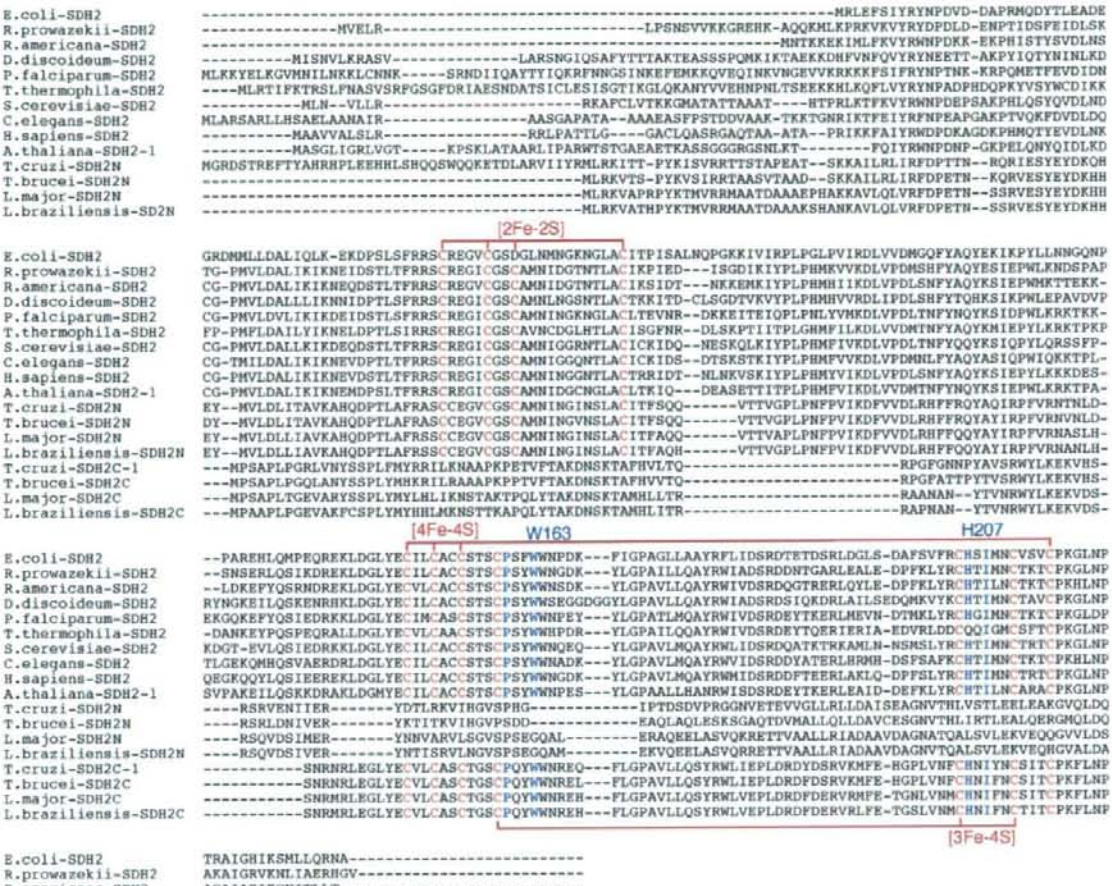

FIGURE 4. **Alignment of heterodimeric SDH2 sequences.** Amino acid residues proposed for binding of the iron-sulfur clusters are shown in *red* and those for the quinone binding in *blue*. Residue numbers refer to the *E. coli* SDH2 (SdhB) sequence. GenBank™ accession numbers for $SDH2_N$ and $SDH2_C$ sequences used are *T. cruzi* (XP_814994 and XP_803796), *T. brucei* (XP_847169 and XP_826981), and *L. major* (XP_001683488 and XP_001682013). Other SDH2 sequences used are *E. coli* (NP_415252), *Rickettsia prowazekii* (Q9ZEA1), *Reclinomonas americana* (NP_044798), *Dictyostelium discoideum* (XP_646559), *Plasmodium falciparum* (D86574), *Tetrahymena thermophila* (XP_001024894), *S. cerevisiae* (NP_012774), *Caenorhabditis elegans* (NP_495992), *H. sapiens* (NP_002991), and *A. thaliana* (NP_189374).

tase activity was monitored in a microplate spectrophotometer (Benchmark Plus, Bio-Rad). Kinetics and UV-visible absorption spectra were determined at room temperature with a V-660 UV-visible spectrophotometer (Jasco, Tokyo, Japan). Protoheme IX and protein concentrations were determined by pyridine hemochromogen method (24) and the micro BCA method (Pierce), respectively. Sequence alignment was done with ClustalX 2.0 (25).

RESULTS AND DISCUSSION

Isolation of T. cruzi Complex II—To determine the molecular organization of *T. cruzi* Complex II, we purified this enzyme from epimastigote mitochondria by ion-exchange and gel filtration chromatography using the nonionic detergent sucrose monolaurate (Table 1). Decylubiquinone-mediated succinate: DCIP reductase activity was eluted as a single peak at each step